CellPress

Nonsense-Mediated mRNA Decay Modulates Immune Receptor Levels to Regulate Plant Antibacterial Defense

Jiradet Gloggnitzer,[1,*] Svetlana Akimcheva,[1] Arunkumar Srinivasan,[2] Branislav Kusenda,[1] Nina Riehs,[1,7] Hansjörg Stampfl,[1] Jaqueline Bautor,[3] Bettina Dekrout,[1] Claudia Jonak,[1] José M. Jiménez-Gómez,[2,4] Jane E. Parker,[3,6] and Karel Riha[1,5,6,*]

[1]Gregor Mendel Institute, Austrian Academy of Sciences, Vienna Biocenter (VBC), Dr.-Bohr-Gasse 3, 1030 Vienna, Austria
[2]Department of Plant Breeding and Genetics
[3]Department of Plant-Microbe Interactions
Max Planck Institute for Plant Breeding Research, Carl-von-Linné-Weg 10, 50829 Cologne, Germany
[4]Institut Jean-Pierre Bourgin, UMR1318, INRA-AgroParisTech, 78000 Versailles, France
[5]CEITEC, Masaryk University, Kamenice 753/5, 625 00 Brno, Czech Republic
[6]Co-senior author
[7]Present address: Department of Biochemistry and Biophysics, University of California, San Francisco, 600 16th Street, San Francisco, CA 94158, USA
*Correspondence: jiradet.gloggnitzer@gmi.oeaw.ac.at (J.G.), karel.riha@ceitec.muni.cz (K.R.)
http://dx.doi.org/10.1016/j.chom.2014.08.010

SUMMARY

Nonsense-mediated mRNA decay (NMD) is a conserved eukaryotic RNA surveillance mechanism that degrades aberrant mRNAs. NMD impairment in *Arabidopsis* is linked to constitutive immune response activation and enhanced antibacterial resistance, but the underlying mechanisms are unknown. Here we show that NMD contributes to innate immunity in *Arabidopsis* by controlling the turnover of numerous TIR domain-containing, nucleotide-binding, leucine-rich repeat (TNL) immune receptor-encoding mRNAs. Autoimmunity resulting from NMD impairment depends on TNL signaling pathway components and can be triggered through deregulation of a single TNL gene, *RPS6*. Bacterial infection of plants causes host-programmed inhibition of NMD, leading to stabilization of NMD-regulated TNL transcripts. Conversely, constitutive NMD activity prevents TNL stabilization and impairs plant defense, demonstrating that host-regulated NMD contributes to disease resistance. Thus, NMD shapes plant innate immunity by controlling the threshold for activation of TNL resistance pathways.

INTRODUCTION

Nonsense-mediated mRNA decay (NMD) is a eukaryotic translation-coupled RNA surveillance mechanism that degrades aberrant mRNA transcripts. Key features of NMD targets are premature termination codons (PTCs) arising as a consequence of mutation, transcription errors, or alternative splicing events (Schweingruber et al., 2013). In mammals, the core NMD machinery relies on the conserved proteins UPF1, UPF2, and

UPF3, which participate in NMD target recognition (Isken and Maquat, 2008). Improper translation termination due to PTCs is thought to recruit UPF1 to stalled ribosomes, which leads to UPF1 phosphorylation (Kashima et al., 2006). Phosphorylated UPF1 facilitates the recruitment of the proteins SMG5, SMG7, and SMG6, which then promote mRNA degradation (Eberle et al., 2009; Okada-Katsuhata et al., 2012; Unterholzner and Izaurralde, 2004). Although UPF1, UPF2, and UPF3 homologs are present in all eukaryotes, homologs of SMG5 and SMG6 appear to be absent from plant genomes (Riehs et al., 2008). Plant and animal NMD target recognition is enhanced by the presence of the exon junction complex (EJC) downstream of PTCs, consisting of the core EJC factors Magoh, Y14, eIFAIII, and Barentsz (Ballut et al., 2005; Nyikó et al., 2013).

Genome-wide analyses showed that up to 20% of endogenous transcripts, including many functional protein-coding as well as noncoding RNAs, are also targeted by NMD due to the presence of NMD-eliciting signatures, including upstream open reading frames (uORFs), long 3′ untranslated regions (UTRs), and introns in 3′ UTRs (Drechsel et al., 2013; Kurihara et al., 2009; Mendell et al., 2004; Weischenfeldt et al., 2008). Thus, beyond its role in RNA surveillance, NMD might also regulate a wide spectrum of biological processes. This is supported by studies in mammalian cells that describe modulation of NMD by various cellular stresses and developmental cues (Bruno et al., 2011; Gardner, 2008; Mendell et al., 2004). Conserved autoregulatory circuits regulate NMD efficiency in mammals and plants, underscoring the importance of precise tuning of NMD to ensure transcriptome homeostasis (Huang et al., 2011; Nyikó et al., 2013; Yepiskoposyan et al., 2011). NMD null mutations are embryonic lethal in *Drosophila*, zebrafish, and mouse, and this has impeded identification of NMD-regulated processes (Hwang and Maquat, 2011). NMD is also essential in plants since disruption of *Arabidopsis* NMD components UPF1 and SMG7 caused seedling death and retarded development, respectively (Arciga-Reyes et al., 2006; Riehs et al., 2008; Yoine et al., 2006). NMD impairment in *Arabidopsis* was linked to constitutive

CrossMark

activation of plant immune responses, characterized by elevated expression of defense genes, production of the plant defense hormone salicylic acid (SA), and enhanced resistance to bacterial infection (Jeong et al., 2011; Rayson et al., 2012; Riehs-Kearnan et al., 2012). Importantly, disruption of disease resistance signaling rescued the adverse effects of *upf1* and *smg7* mutations (Riehs-Kearnan et al., 2012). Thus, aberrant pathogen response signaling is a major physiological consequence of impaired NMD in *Arabidopsis*, suggesting a role for NMD in regulating plant immunity.

The plant innate immune system employs successive defense layers to inhibit pathogen infection. One defense layer relies on plasma membrane-localized receptors that detect conserved pathogen-associated molecular patterns (PAMPs). Recognition of PAMPs triggers transcriptional reprogramming, known as PAMP-triggered immunity (PTI), that is sufficient to confer resistance against nonadapted pathogens (Jones and Dangl, 2006). Infectious (virulent) pathogenic strains deliver a battery of effectors to host cells to interfere with defense programs. However, these pathogens encounter a postinfection resistance barrier (hereafter referred to as postinfection basal resistance or immunity), controlled by intracellular complexes of the immune regulators EDS1 and PAD4, which reinstate resistance to slow infection (Rietz et al., 2011), in part via the SA defense signaling pathway (Fu and Dong, 2013). Basal resistance to virulent pathogens is further reinforced by intracellular nucleotide-binding, leucine-rich repeat (NLR) receptors, which detect the presence or actions of specific pathogen effector proteins to confer effector-triggered immunity (ETI) (Dodds and Rathjen, 2010). NLRs represent one of the largest and most variable plant gene families that have undergone rapid evolutionary diversification, likely driven by pathogens (Guo et al., 2011). ETI engages components of the basal resistance machinery to amplify defense programs, often culminating in programmed cell death at local infection sites, which is also known as the hypersensitive response (HR) (Maekawa et al., 2011). Plant NLRs are broadly divided into two subclasses carrying an N-terminal Toll/inter-leukin-1 receptor (TIR) domain or a coiled-coil (CC) domain (referred to, respectively, as TNLs and CNLs), with genetically distinct signaling requirements (Heidrich et al., 2012). The expression of NLRs is tightly regulated at transcriptional and posttranscriptional levels (Staiger et al., 2013), and NLR misexpression often triggers autoimmunity associated with severe stunting and fitness costs (Alcázar and Parker, 2011).

Here we elucidate the mechanism underlying autoimmunity caused by NMD deficiency in *Arabidopsis*. We show that autoimmune phenotypes associated with SMG7 dysfunction are due to TNL receptor transcript misregulation and that host-modulated NMD dynamically regulates the abundance of TNL receptors, thus influencing immune response thresholds. We conclude that NMD represents a physiological gene regulatory mechanism contributing to plant innate immunity.

RESULTS

### Genetic Requirements of *smg7* Autoimmunity
Arabidopsis accession Columbia (Col) carrying the loss-of-function *smg7-1* mutation (hereafter referred to as *smg7*) exhibits autoimmunity, characterized by stunting, spontaneous formation

of necrotic lesions, and elevated SA levels. The *smg7* aberrant phenotypes were suppressed by mutations in the basal and TNL immunity regulator *PAD4* (Figures 1A, 1B, and S1A). By contrast, defects in a CNL receptor signaling component, NDR1, did not rescue the *smg7* mutant (Riehs-Kearnan et al., 2012). We explored further the genetic basis for NMD autoimmunity by crossing *smg7* with a loss-of-function mutant of the key basal and TNL immunity regulator EDS1. Mutation of *EDS1* fully suppressed *smg7* stunting and expression of the SA-responsive marker gene *PR1* (Figures 1A, 1B, and S1A). Combinations of *smg7* with mutations in the HSP90 cochaperones *RAR1* and *SGT1b*, which assist the activation of many NLR receptor complexes (Kadota et al., 2010), also suppressed *smg7* stunting and strongly reduced *PR1* expression, but retained some altered *smg7* leaf morphology (Figures 1A, 1B, and S1A). Notably, inhibition of SA biosynthesis by mutation of *ICS1/SID2* did not suppress *smg7* stunting, but reduced *PR1* expression and chlorosis (Figures 1A, 1B, and S1C). The above *smg7* genetic requirements point to involvement of TNL receptor signaling in *smg7* autoimmunity, since TNLs immediately engage EDS1/PAD4 basal immunity signaling components (Heidrich et al., 2011; Rietz et al., 2011; Wagner et al., 2013). This is further supported by the suppression of autoimmunity in *smg7* plants grown at 28°C compared to 21°C (Figures 1D, 1E, and S1B), because TNL resistance is temperature sensitive (Alcázar and Parker, 2011). By contrast, early PTI defense signaling outputs, such as generation of reactive oxygen species (ROS) and induction of PTI marker genes *FRK1* and *WRKY29* upon treatment with the flagellin-derived PAMP elicitor flg22, were unaltered in *smg7* and *smg7 pad4* plants, despite the fact that *smg7* plants showed elevated *FRK1* steady-state levels (Figures S1D and S1E). We also tested growth in plants of virulent *Pseudomonas syringae pv tomato* (*Pst*) DC3000 and the type III secretion-defective *Pst* DC3000 *hrcC⁻* strain, which fails to inject effector proteins into host cells to suppress PTI (Dodds and Rathjen, 2010). While *smg7* mutants were highly resistant to virulent *Pst* DC3000 and *Pst* DC3000 *hrcC⁻* compared to wild-type, enhanced resistance was abolished in *smg7 pad4* plants (Figure S1F). These data suggested that increased resistance of *smg7* mutants to virulent *Pst* DC3000 and *Pst* DC3000 *hrcC⁻* depends on *PAD4*, consistent with its role in basal and TNL resistance (Rietz et al., 2011). The above findings further substantiate a role for NMD in TNL receptor regulation, but not in early PTI responses to pathogens.

Next, we examined whether alleviation of *smg7* autoimmunity in certain resistance signaling mutant backgrounds could be explained by restored NMD efficiency. For this, we measured the accumulation of endogenous PTC-containing (PTC+) splice variants of *RS2Z33* and AT2G45670 that are targeted by NMD (Kalyna et al., 2012). Aberrant PTC+ mRNA levels were increased in all *smg7* immunity mutant backgrounds (Figure 1C), as well as in *smg7* plants grown at 28°C or 21°C (Figure 1F). Therefore, suppression of TNL resistance pathways does not alter the NMD defect in *smg7* but rather the consequences of altered NMD efficiency.

Stability of TNL Receptor Transcripts Is Directly Regulated by NMD
Since reduced NMD leads to autoimmunity, we asked whether NMD controls the expression of immunity-related transcripts.
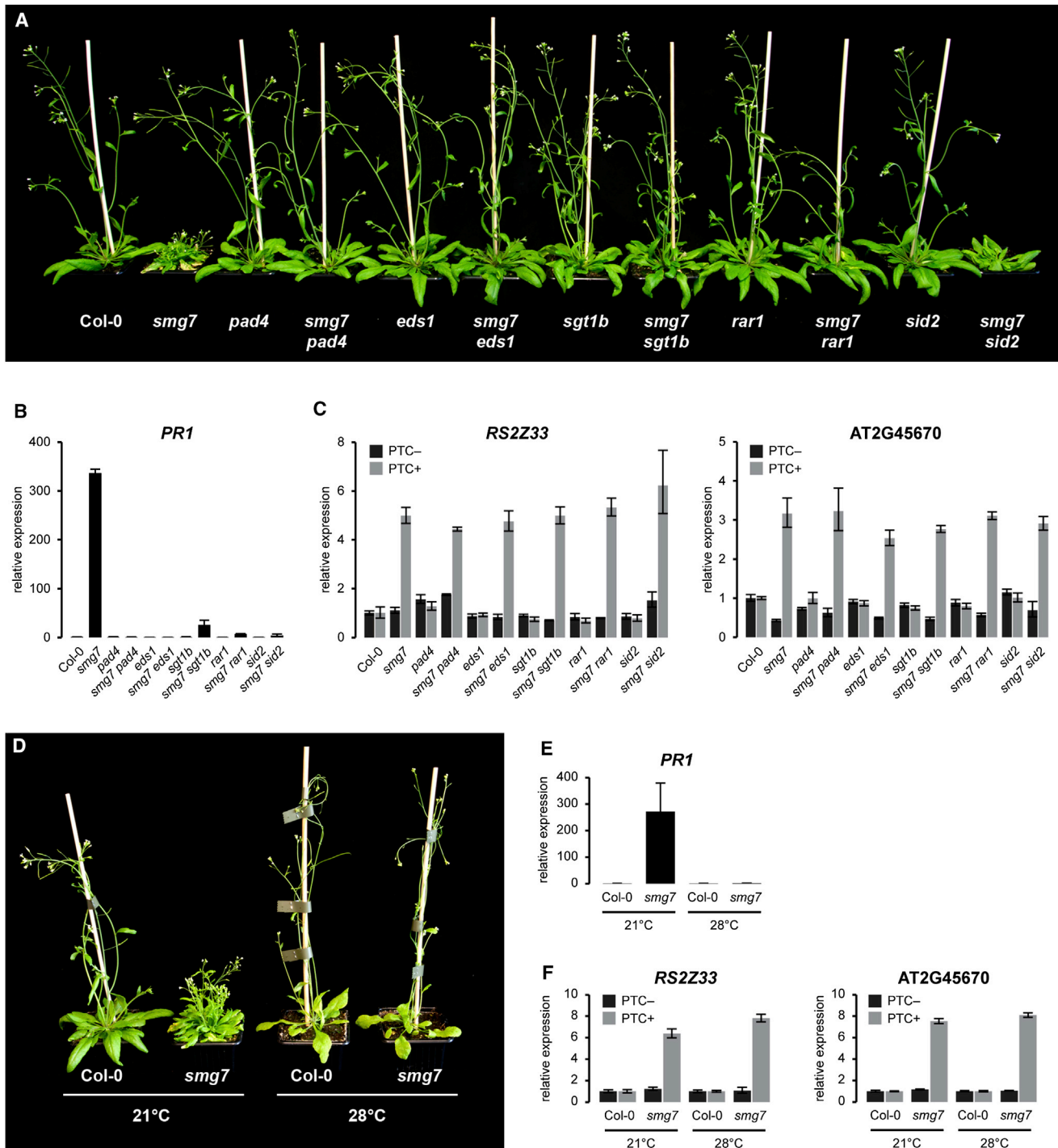
Figure 1. *Smg7* Autoimmunity Is Conditioned by TNL Signaling Components

(A) Morphology of 5-week-old plants of the indicated genotypes.

(B) *PR1* expression measured by qRT-PCR in the indicated genotypes.

(C) Expression of PTC−/+ splice variants of NMD reporters *RS2Z33* and AT2G45670 in the indicated genotypes.

(D) Morphology of 5-week-old Col and *smg7* plants grown at 21°C and 28°C.

(E) *PR1* expression in plants shown in (D).

(F) Expression of NMD reporters *RS2Z33* and AT2G45670 in plants shown in (D).

Expression levels in (B), (C), (E), and (F) are mean ± standard error of mean (SEM) of four biological replicates. See also Figure S1.

Published whole-genome expression data in NMD-impaired *Arabidopsis* mutants showed that altered NMD affects a significant portion of the transcriptome (Drechsel et al., 2013; Kurihara et al., 2009), but developmental abnormalities of these mutants impede identification of direct NMD targets. To avoid this problem, we performed RNA-seq analysis of *smg7 pad4* mutants that develop normally due to the block in immunity signaling (Figure 1A). Of 17,269 mRNAs expressed in leaf tissues, 2,653 mRNAs (~15%) were significantly upregulated in *smg7 pad4* compared to *pad4* control plants (false discovery rate corrected p value *q* < 0.05; Figures 2A and S2A and Table S1). Gene Ontology (GO)-term classification of upregulated transcripts showed no enrichment for the category "response to abiotic or biotic stimulus" (Fisher's exact test, p = 0.1193; Figure S2B), consistent with abrogated defense signaling in *pad4* and showing that NMD-regulated transcripts are broadly distributed across all GO-term categories. In addition, comparison of *smg7 pad4* upregulated transcripts (1.8-fold threshold) revealed substantial overlap with expression data of two weak NMD mutants, *upf1-1* and *upf3-1*, which exhibit extremely mild autoimmune phenotypes (Kurihara et al., 2009) (Figure S2C). We then examined the RNA-seq data for differences in the expression of NLRs. *Arabidopsis* accession Col contains 110 annotated TNLs and 59 CNLs (Meyers et al., 2003), of which 72 TNLs and 42 CNLs were expressed in our RNA-seq data set (Table S2). Thirty-nine expressed TNLs and 11 CNLs were upregulated in *smg7 pad4* mutants, representing a statistically significant enrichment of TNL transcripts in the absence of autoimmunity (Fisher's exact test, p = 5.329^{-16}), while CNL transcripts were not significantly enriched (p = 0.155) (Figures 2B and S2D). Based on transcript annotations (TAIR 10 and by Tan et al. [2007]), we established that ~50% of the upregulated TNLs carry putative NMD features (Figure S2E and Table S2). By contrast, canonical NMD features were absent in upregulated CNLs, suggesting that they are not NMD targets (Table S2). We validated the RNA-seq trends by measuring steady-state levels of selected TNL and CNL transcripts by qRT-PCR in *smg7 pad4* and *pad4* leaves (Figures 2C and S2F). Among the *smg7 pad4* upregulated TNLs, we identified *RPS6* that was reported to undergo alternative splicing (Kim et al., 2009). We found that a subset of *RPS6* PTC+ splice variants was upregulated in *smg7 pad4*, indicating regulation by NMD (Figure S2G). Transcript levels of other selected TNLs were also increased in wild-type plants treated with the NMD and translation inhibitor cycloheximide (Figure 2D). To determine whether TNL and CNL transcripts are regulated by NMD, we assessed their mRNA degradation kinetics after imposing a transcriptional block (Johnson et al., 2000). Similar to the PTC+ splice variants of NMD reporters AT2G45670 and RS2Z33, we found increased half-lives for all tested TNL transcripts in *smg7 pad4* plants, with the exception of AT1G72940, which is likely to be transcriptionally regulated (Figure 2E). In agreement with previous studies in mammalian cells, most NMD-targeted TNLs and NMD control transcripts showed biphasic degradation kinetics (Trcek et al., 2013). By contrast, *smg7 pad4* upregulated CNLs did not display changes in half-lives, suggesting that they are not processed by NMD (Figure S2H). Taken together, our results show that NMD specifically targets a large subset of TNL receptor transcripts.

A Natural Variant of TNL *RPS6* Confers Autoimmunity in NMD-Impaired Plants

Given the extensive natural variation in NLR repertoires across *Arabidopsis* accessions (Guo et al., 2011), we examined the impact of a different genetic background, that of accession Landsberg *erecta* (L*er*), on *smg7* autoimmunity. When we crossed Col *smg7* with L*er*, we found that stunting was suppressed in a portion of recombinant F2 *smg7* Col/L*er* progeny, suggesting the existence of natural polymorphism(s) affecting constitutive resistance (Figures S3A and S3B). Since introgression of the *smg7* mutation into a L*er* background by four further crosses to L*er* completely restored the stunting phenotype (Figures S3A and S3C), we concluded that the suppression of *smg7* autoimmunity in the F2 population arises out of a combination of Col and L*er* polymorphisms at multiple genetic loci. Genetic analysis of the L*er*-derived *smg7* suppressors pointed to the existence of at least two independent suppressor loci that displayed recombination suppression, impeding further mapping. However, we found that the suppressor phenotype of *smg7* plants in L*er* (hereafter referred to as L*er*-*smg7* plants) was determined by a single Col locus, denoted *REX* (*RIESENEXPERIMENT*) (Figures 3A, S3A, and S3C).

While L*er*-*smg7* plants harboring $REX^{Ler/Ler}$ exhibited hallmarks of autoimmunity, L*er*-*smg7* plants carrying the $REX^{Col/Col}$ suppressor locus did not exhibit constitutive resistance signaling (Figures 3A–3C). The REX^{Ler} allele was semidominant, consistent with a model in which L*er*-*smg7* autoimmunity is conferred by the REX^{Ler} locus in a dose-dependent manner (Figures 3A–3C). Since NMD reporter levels increased in L*er*-*smg7* mutants irrespective of the *REX* allele present, we concluded that *REX* does not encode an NMD modifier (Figure 3D). We mapped the *REX* locus to a 240 kb region on chromosome 5, encompassing 60 genes between AT5G46520 and AT5G46850 in the L*er* reference sequence, including disease resistance signaling genes and several TNLs (Figure 3E). RNA-seq analysis of L*er*-*SMG7* $REX^{Ler/Ler}$ and L*er*-*smg7* $REX^{Ler/Ler}$ plants revealed that of six TNL genes in the REX^{Ler} region, three (*RPS6*, AT5G46490, and AT5G46500) were overexpressed in L*er*-*smg7* $REX^{Ler/Ler}$ plants compared to L*er*-*SMG7* $REX^{Ler/Ler}$ (Figure 3F). To identify the causative TNL, we transformed wild-type-appearing L*er*-$SMG7^{+/-}$ $REX^{Col/Col}$ plants with genomic constructs of upregulated candidate TNLs and scored transformed L*er*-*smg7* $REX^{Col/Col}$ T2 progeny for autoimmunity. L*er*-*smg7* $REX^{Col/Col}$ plants transformed with $RPS6^{Ler}$ displayed autoimmunity, but segregating *SMG7* siblings did not (Figures 4A and 4B; 9 out of 11 independent transgenic lines). Also, $RPS6^{Ler}$ mRNA levels increased in L*er*-*smg7* transformants but not in transformed *SMG7* siblings (Figure 4C). These results suggest that the TNL $RPS6^{Ler}$ locus underlies L*er*-*smg7* autoimmunity in an NMD deficiency-dependent manner.

Both $RPS6^{Ler}$ and $RPS6^{Col}$ transcripts are NMD targets since their levels increased similarly upon NMD inhibition by cycloheximide (Figure S4A). Therefore, the $RPS6^{Ler}$-conditioned autoimmunity in L*er*-*smg7* plants is not explained by its specific targeting for NMD. The $RPS6^{Ler}$ allele harbors one in-frame INDEL and six nonsynonymous mutations in the coding region, but none were within conserved TNL motifs such as the P-loop, Walker B, or MHD motifs that would account for a functional difference between $RPS6^{Col}$ and $RPS6^{Ler}$ (Figure 4D). Additionally, no
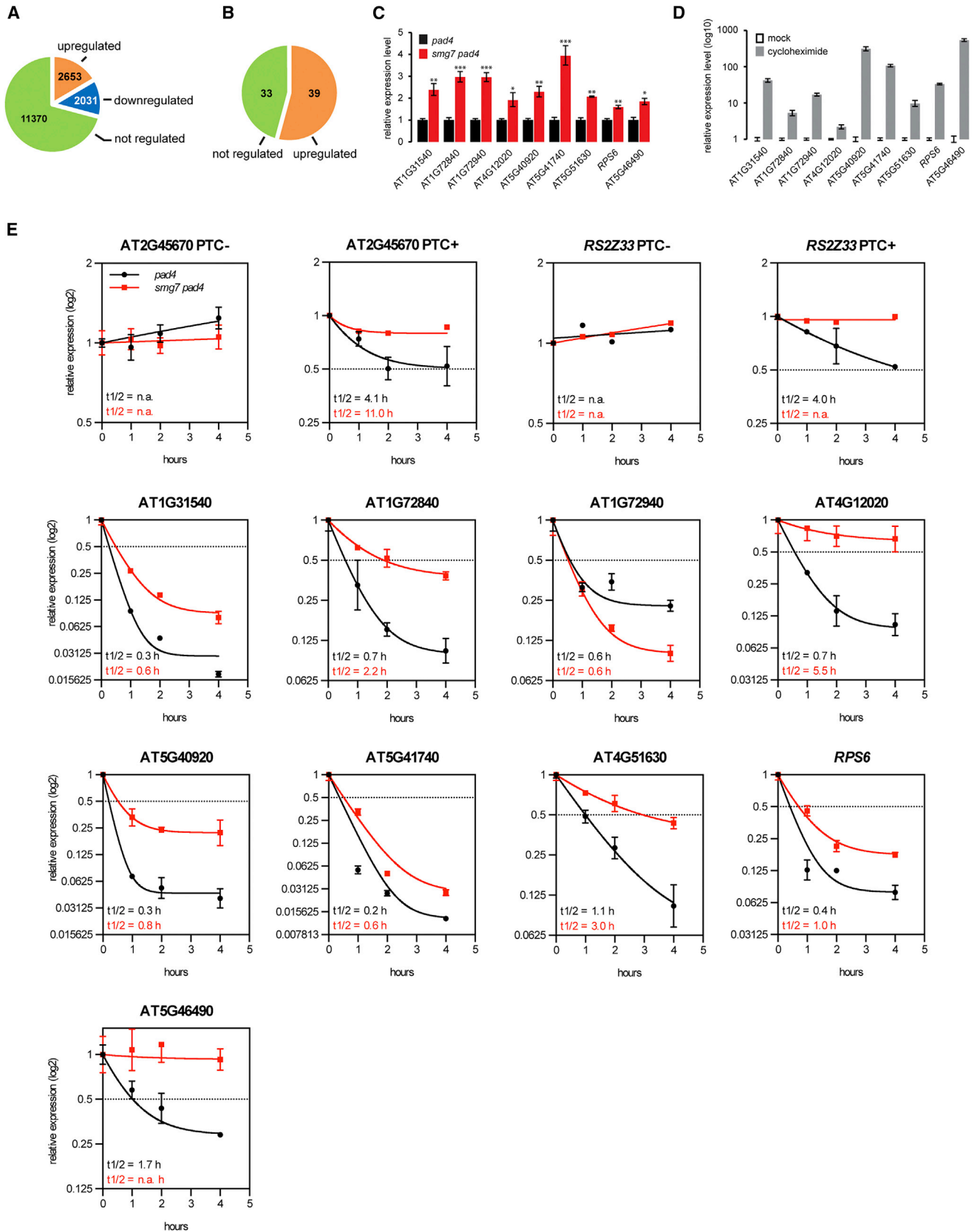
polymorphism was predicted to affect splice donor or acceptor sites. Previously, a survey of 32 *Arabidopsis* accessions revealed *RPS6*-conditioned natural variation in immune responses to *Pst* effector HopA1. Some *RPS6* alleles, including *RPS6*^{Ler}, induced a pronounced HR upon HopA1 effector recognition, while this was not the case for *RPS6*^{Col} (Gassmann, 2005). In agreement, we found that L*er*-*SMG7 REX*$^{Ler/Ler}$ plants inoculated with *Pst* DC3000-HopA1 displayed a strong HR, whereas L*er*-*SMG7 REX*$^{Col/Col}$ plants produced no macroscopically discernable HR (Figure S4B). These data suggest that autoimmunity in L*er*-*smg7 REX*$^{Ler/Ler}$ plants is caused by derepression of *RPS6*^{Ler}, which induces a strong HR. Collectively, the data show that naturally occurring variation in TNLs can influence immunity and cell death thresholds in NMD-deficient plants, and that in certain genetic backgrounds deregulation of a single NMD-regulated TNL is sufficient to trigger autoimmunity.

Virulent Bacterial Pathogen Infection Reduces NMD Efficiency

Inappropriate activation of immune responses in *Arabidopsis* NMD mutants leads to increased resistance against infectious bacterial pathogens (Jeong et al., 2011; Rayson et al., 2012; Riehs-Kearnan et al., 2012). Therefore, we asked whether NMD efficiency is itself modulated in response to pathogen infection, as a possible target for pathogen interference and/or means for the plant to promote resistance. To test this, we spray-inoculated Col wild-type plants with virulent *Pst* DC3000 and measured the effect on endogenous NMD targets. Coinciding with increased *PR1* levels at 48–72 hr postinoculation (hpi) (Figure 5A), we observed elevated transcript levels of NMD factors *SMG7* and *BARENTSZ1* at 48 and 72 hpi and an increase in *RS2Z33* PTC+ at 72 hpi (Figure 5A). Since *SMG7* and *BARENTSZ1* levels are autoregulated by NMD, their increased accumulation reflects decreased NMD efficiency (Nyikó et al., 2013). Expression of several NMD-targeted TNLs, including *RPS6*, was also increased at 72 hpi (Figure 5A). We then examined transcript stability in order to discern whether upregulation of the NMD targets was a result of impaired NMD. Analysis of mRNA decay rates upon imposing a transcriptional block 72 hr after *Pst* DC3000 infection revealed that half-lives of NMD reporters and NMD-targeted TNLs increased after *Pst* DC3000 inoculation compared to mock treatment (Figure 5B). Therefore, we concluded that NMD target upregulation was a result of impaired NMD. In line with our previous analysis of TNL stability in *smg7 pad4* plants (Figure 2E), the decay rate of TNL AT1G72940 did not change after *Pst* DC3000 treatment (Figure 5B), arguing that its increased expression was due to increased transcription. We concluded that virulent bacterial infection leads to reduced NMD and thus stabilization of NMD targets, including TNL transcripts.

To test whether NMD inhibition is a result of pathogen effector activities targeting NMD or is part of an intrinsic host defense program, we inoculated wild-type plants with virulent *Pst* DC3000 or *Pst* DC3000 *hrcC*$^-$ strain that triggers strong PTI. We used leaf syringe infiltration for both strains because the *Pst* DC3000 *hrcC*$^-$ strain grows poorly on wild-type plants. Transcripts of *SMG7*, *RS2Z33* PTC+, and the TNL *RPS6* were upregulated at 24–48 hpi in response to *Pst* DC3000 and *Pst* DC3000 *hrcC*$^-$ (Figure 6A). Similar expression trends were observed after treatment of wild-type seedlings with the PAMP-elicitor flg22 (Figure 6B). Because PAMP perception alone reduced NMD, we concluded that NMD suppression is an integral part of the host-programmed immune response.

Previous studies in mammalian cells showed that stress-induced phosphorylation of the eukaryotic translation initiation factor eIF2α by GCN2 kinase, for example, upon amino acid starvation, leads to inhibition of translation and thus suppression of NMD (Mendell et al., 2004). We therefore tested if GCN2-dependent phosphorylation of eIF2α inhibits NMD in *Arabidopsis*. Amino acid starvation led to NMD suppression in both Col and *gcn2-2* mutant seedlings, suggesting that GCN2 is not required for NMD inhibition (Figures S5A and S5B). Similarly, the *gcn2-2* mutation did not abolish NMD inhibition when we spray-inoculated plants with virulent *Pst* DC3000 bacteria (Figure S5C). Furthermore, *gcn2-2* mutants did not have altered basal resistance to virulent *Pst* DC3000 (Figure S5D), arguing that GCN2-dependent phosphorylation of eIF2α is dispensable for stress-induced NMD inhibition and does not contribute to immune responses.

Disruption of *SMG7* Autoregulation Sensitizes Plants to Infection

We reasoned that dampening of NMD upon bacterial pathogen infection might represent a physiological mechanism for bolstering defenses. If this were the case, failure to suppress NMD during infection would lead to increased disease susceptibility. To test this, we generated *smg7* mutants expressing *SMG7* cDNA from an actin promoter. The *SMG7* construct lacked an endogenous *SMG7* 3′ UTR with introns, rendering its transcript insensitive to NMD autoregulation (*SMG7-ΔUTR*). The *SMG7-ΔUTR* transgene fully complemented *smg7* autoimmunity in two independent lines (Figures 7A, 7B, S6A, and S6B). Both lines expressed ∼2-fold higher *SMG7* mRNA levels (Figures 7B and S6C) than wild-type and had lower levels of multiple NMD targets, demonstrating increased NMD efficiency (Figures 7B, S6D, and S6E).

Figure 2. NMD Targets TNL Transcripts
(A) Classification of significantly upregulated (adjusted p value $q < 0.05$), downregulated ($q < 0.05$), or not significantly changed transcripts ($q \geq 0.05$) in *smg7 pad4* relative to *pad4* control plants. The number of transcripts in each category is indicated.
(B) Classification of significantly upregulated ($q < 0.05$) or expressed but not significantly changed TNL transcripts ($q \geq 0.05$) in *smg7 pad4* relative to *pad4* plants. The number of transcripts in each category is indicated.
(C) Steady-state levels of selected TNL transcripts in *pad4* and *smg7 pad4* measured by qRT-PCR (mean ± SEM, three biological replicates). Significant differences (*p < 0.05, **p < 0.01, ***p < 0.001) compared to *pad4* control samples are indicated (two-tailed Student's t test).
(D) Expression of selected TNL transcripts 5 hr after translational inhibition with cycloheximide in wild-type plants (mean ± SEM, three biological replicates).
(E) qRT-PCR analysis of half-lives of TNL transcripts and NMD reporters AT2G45670 and *RS2Z33* in *pad4* and *smg7 pad4*. Half-lives ($t_{1/2}$) were calculated by nonlinear least-square regression (data points are mean ± SEM, three biological replicates). The experiment was repeated twice with similar results.
See also Figure S2 and Tables S1 and S2.
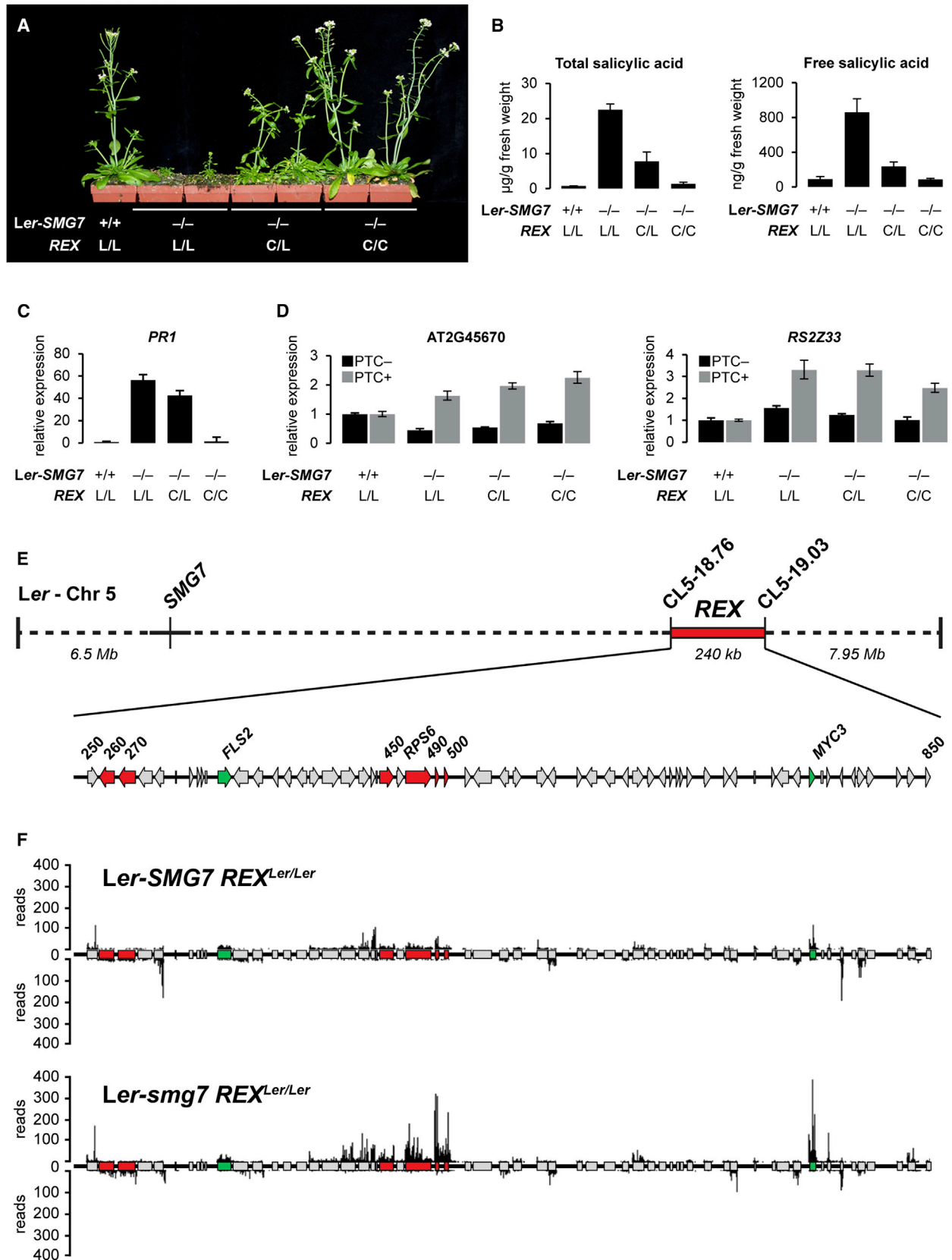
(legend on next page)
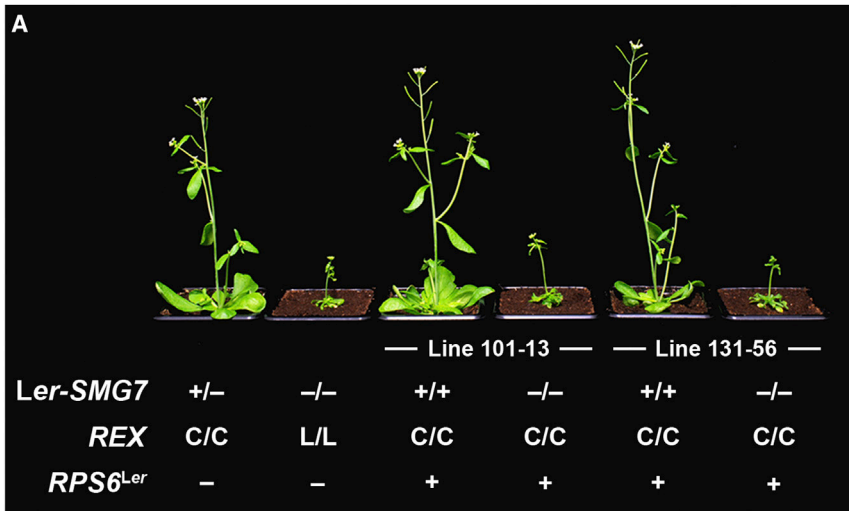
Figure 4. The TNL *RPS6* Underlies L*er*-smg7 Autoimmunity

(A) Independent T2 progeny lines 101-13 and 131-56 derived from L*er*-*SMG7*^{+/−} plants harboring *REX*[Col/Col] (left) transformed with a genomic construct of *RPS6*[Ler]. L*er*-smg7 *REX*[Ler/Ler] plants (second to the left) are shown as control for the stunting phenotype. The allelic variant of *REX* is indicated with "L" (L*er*) or "C" (Col). L*er*-*SMG7*^{+/−} control plants are shown on the left.

(B) *PR1* expression in plants shown in (A).

(C) Total levels of *RPS6* transcripts (derived from Col and L*er* alleles) in plants shown in (A). Asterisks indicate significant differences (**p < 0.01, ***p < 0.001) to L*er*-*SMG7*^{+/−} *REX*[Col/Col] (two-tailed Student's t test).

(D) Domain organization and exon/intron structure in *RPS6*[Col]. The depicted polymorphisms were identified in *RPS6*[Ler] by Sanger sequencing.

Values shown in (B) and (C) are mean ± SEM of four biological replicates. See also Figure S4.
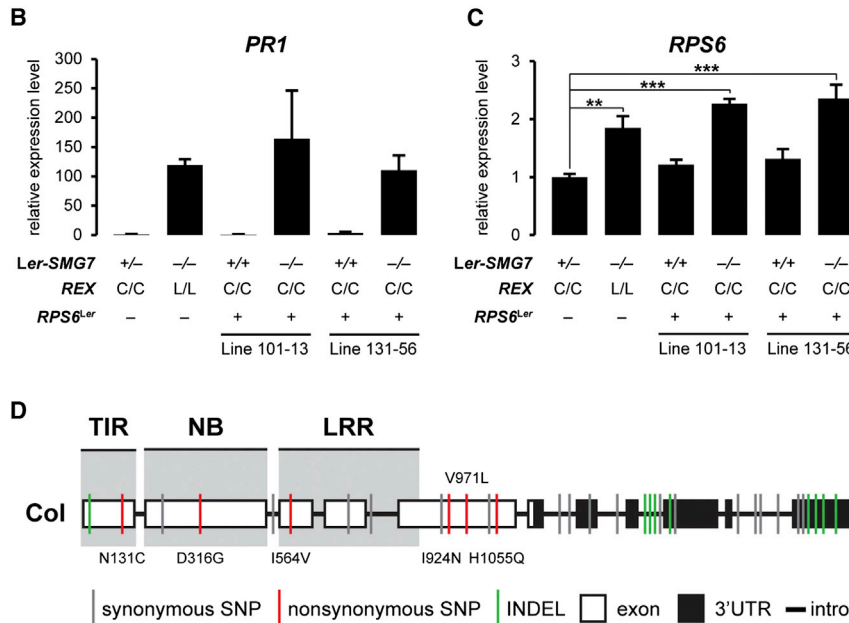
RS2Z33 PTC+ and NMD-targeted TNL mRNAs AT5G40920 and *RPS6* upon *Pst* DC3000 infection (Figures 7D and S6G). However, *PR1* induction was unaffected in *SMG7-ΔUTR* plants, suggesting that SA-dependent defense responses are not altered by constitutive NMD activation (Figures 7E and S6H). Similarly, the induction of PTI marker genes *WRKY29* and *FRK1* and generation of ROS upon flg22 treatment remained unaffected in *SMG7-ΔUTR* plants (Figures S6I and S6J). Our data show that removal of *SMG7* autoregulatory elements increases NMD efficiency and prevents NMD inhibition upon *Pst* DC3000 infection without affecting early PTI or SA-dependent outputs.

We then determined whether the failure to suppress NMD in *SMG7-ΔUTR* plants impacts disease resistance by comparing *Pst* DC3000 and *Pst* DC3000 *hrcC*[−] growth in wild-type and *SMG7-ΔUTR* plants. Similar to *eds1-2* mutants, *SMG7-ΔUTR* plants supported significantly higher *Pst* DC3000 bacterial titers than wild-type at 3 days postinoculation, while low *Pst* DC3000 *hrcC*[−] growth remained unaffected in *SMG7-ΔUTR plants*

We next tested whether expression of *SMG7-ΔUTR* influenced NMD regulation after bacterial infection. Whereas spray inoculation of wild-type plants with virulent *Pst* DC3000 led to a 2-fold increase in *SMG7* mRNA, *SMG7* transcript levels in *SMG7-ΔUTR* plants remained constant (Figures 7C and S6F). Unlike wild-type, *SMG7-ΔUTR* plants did not upregulate

Figure 3. The *REX*[Ler] Locus Underlies Autoimmunity in L*er*-smg7 Mutants

(A) Five-week-old *smg7* plants in L*er* genomic background (L*er*-smg7) carrying either Col (C) or L*er* (L) alleles of *REX*. L*er*-*SMG7* control plants are shown on the left.

(B) Quantification of total and free SA of plants shown in (A) (mean ± standard deviation, three biological replicates).

(C) *PR1* expression in plants shown in (A).

(D) NMD reporter expression in plants shown in (A).

(E) Genetic map of L*er* chromosome 5. The *REX* locus is indicated by a red bar, located between markers CL5-18.76 and CL5-19.0 (Table S4). Genes are shown as arrows (TNL genes in red, other pathogen responsive genes in green). The three digits next to the genes are identifiers for the last corresponding AGI numbers (AT5G46XXX).

(F) Normalized RNA-seq read profiles mapping to *REX*[Ler] in L*er*-*SMG7* and L*er*-smg7 plants.

Values shown in (C) and (D) are mean ± SEM of four biological replicates. See also Figure S3.
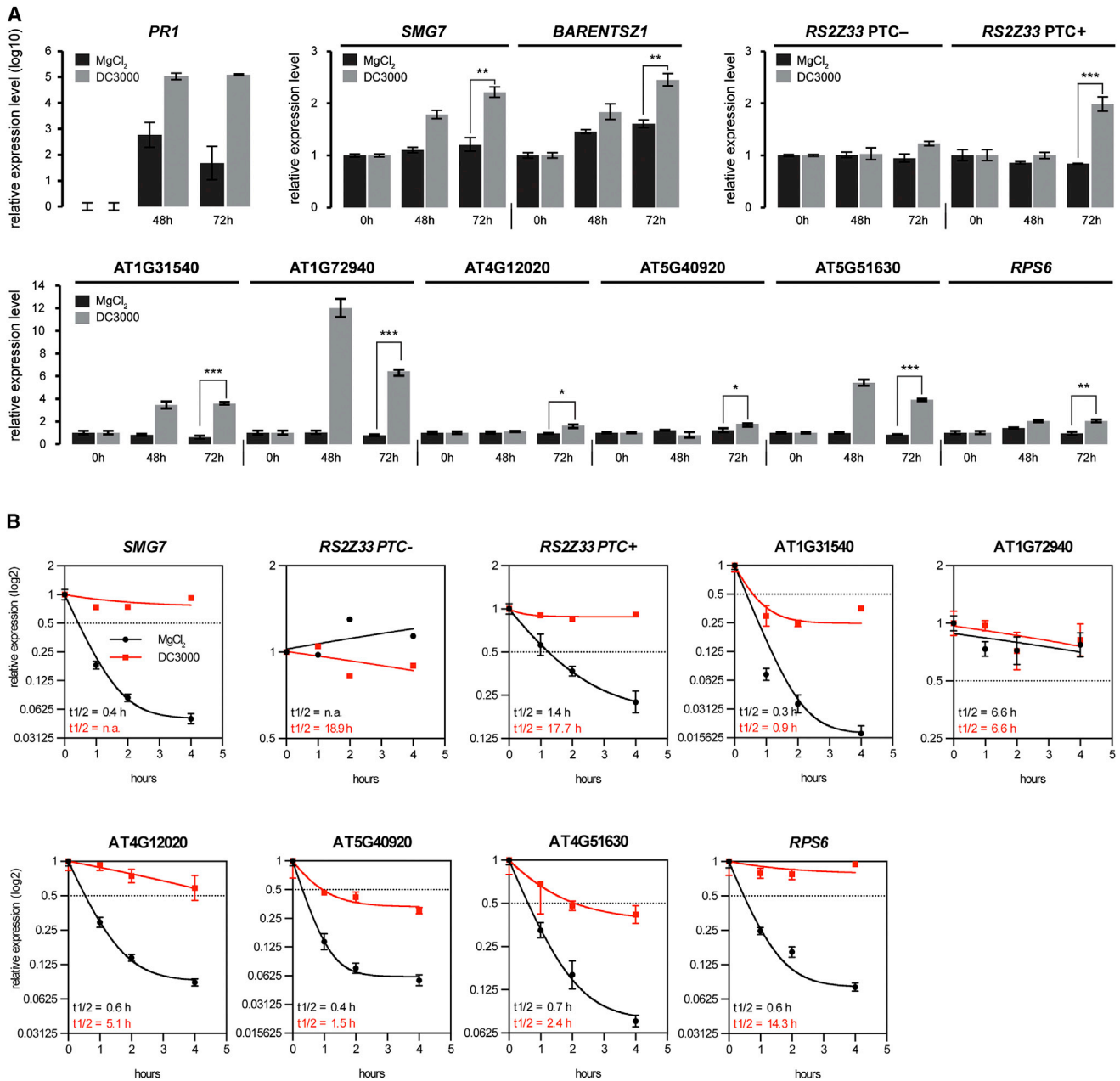
Figure 5. NMD Efficiency Declines upon Pathogen Infection

(A) Expression of *PR1*, NMD factors *SMG7* and *BARENTSZ1*, the NMD reporter *RS2Z33*, and selected TNLs in wild-type plants after treatment with *Pst* DC3000 or mock (MgCl₂) (mean ± SEM of three biological replicates, normalized to 0 hpi). Asterisks indicate significant differences (*p < 0.05, **p < 0.01, ***p < 0.001) to mock treatment at the respective time point (two-tailed Student's t test).

(B) qRT-PCR analysis of half-lives of selected TNL transcripts and NMD reporters AT2G45670 and *RS2Z33* after treatment with *Pst* DC3000 or mock. Data points are mean ± SEM of three biological replicates.

Experiments shown in (A) and (B) were repeated three times with similar results. See also Figure S5.

(Figure 7F). The increased susceptibility of *SMG7-ΔUTR* plants to virulent *Pst* DC3000, together with the normal PTI responses observed in these lines, supports the idea that host-directed suppression of NMD contributes to postinfection basal resistance mechanisms downstream of early PTI responses.

DISCUSSION

An increasing body of evidence suggests that, beyond its role in mRNA surveillance, NMD is also important for regulating physiological gene expression. For example, NMD efficiency was reported to vary between cell types and tissues and in response
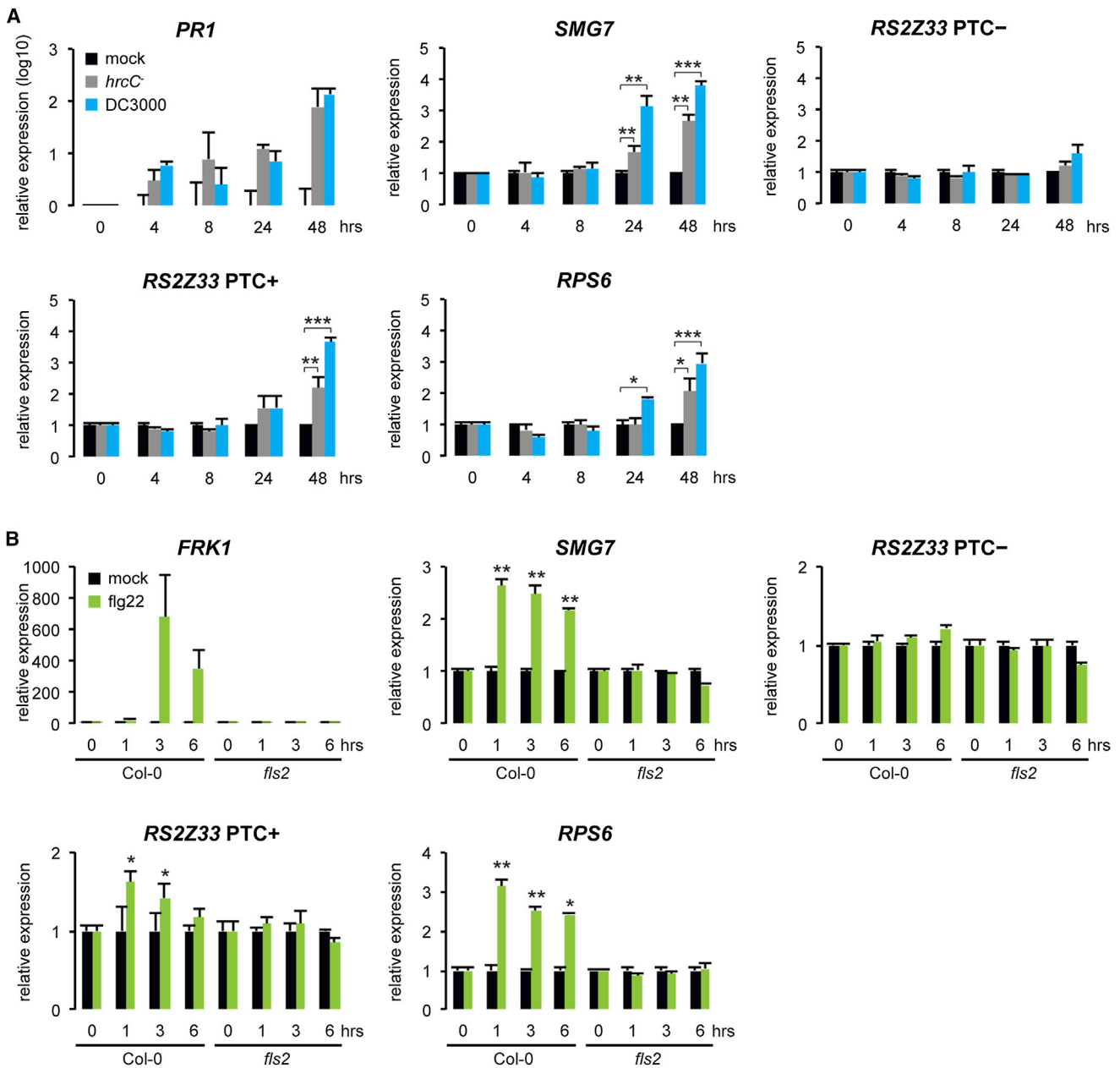
Figure 6. PAMP Perception Dampens NMD

(A) Expression of *SMG7*, NMD reporter *RS2Z33*, and TNL AT5G40920 upon syringe infiltration with *Pst* DC3000 and *Pst* DC3000 *hrcC⁻* (mean ± SEM of four biological replicates). *PR1* expression serves as a marker for SA-dependent defense responses.

(B) Expression of *SMG7*, NMD reporter *RS2Z33*, and TNL AT5G40920 upon flg22 treatment (1 μM) of wild-type and *fls2* seedlings, which serve as a negative control for flg22-induced responses (mean ± SEM of three biological replicates). *FRK1* expression serves as a marker for PTI induction.

Expression values in (A) and (B) were normalized to mock treatment at the respective time point. Asterisks indicate significant differences (*p < 0.05, **p < 0.01, ***p < 0.001) compared to mock (two-tailed Student's t test). Both experiments were repeated with similar results.

to cellular stress (Karam et al., 2013). Most studies describe a decline in NMD efficiency during cell differentiation or exposure to stresses (Bruno et al., 2011; Gardner, 2008; Mendell et al., 2004), suggesting that relaxed RNA surveillance might promote the expression of genes involved in development or stress adaptation (Karam et al., 2013). However, the significance of this regulation is unknown. Also, approaches to identify biologically relevant NMD targets have largely drawn correlations between functional annotations of candidate NMD transcripts and expression, leaving causal relationships unclear (Karam et al., 2013). Here we identify a causal link between NMD impairment and pathogen resistance in *Arabidopsis* and show that NMD surveillance is an integral part of the plant immune response. We establish that NMD regulates the turnover of multiple TNL
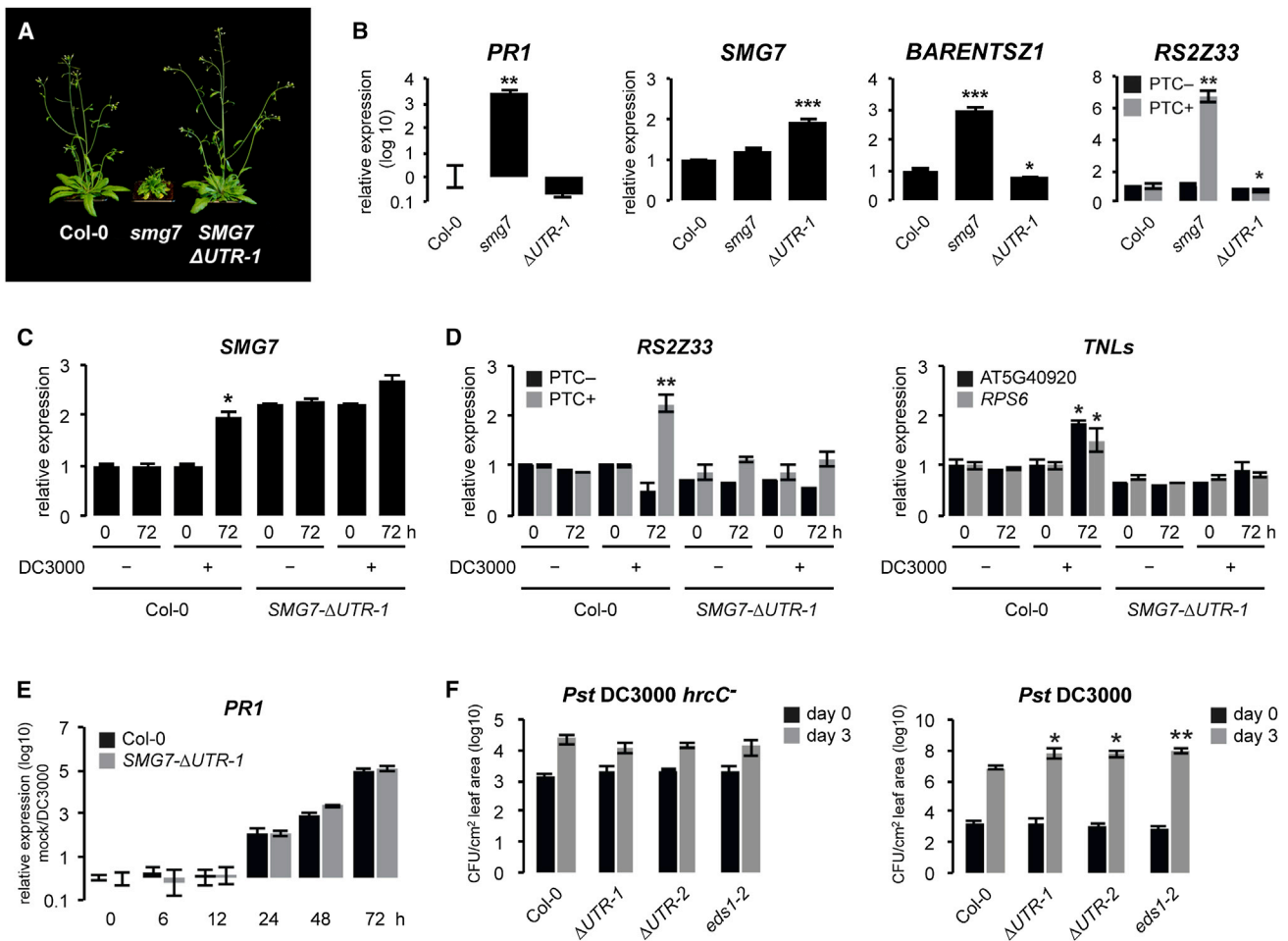
Figure 7. Impairment of NMD Autoregulation Reduces Basal Resistance

(A) Five-week-old Col, smg7, and a transgenic smg7 mutant line complemented with SMG7 cDNA lacking the endogenous 3′ UTR (SMG7-ΔUTR-1) are shown.

(B) PR1, SMG7, and BARENTSZ1 expression in plants shown in (A) (mean ± SEM, four biological replicates). Values for SMG7 in SMG7-ΔUTR plants are total levels of endogenous SMG7 and SMG7-ΔUTR transgene.

(C and D) Expression of SMG7, RS2Z33, and TNLs RPS6 and AT5G40920 in Col and SMG7-ΔUTR-1 plants after spray inoculation with Pst DC3000 (+) or mock inoculation with MgCl₂ (−). Values are averages of three biological replicates (±SEM) and are relative to Col levels at 0 hpi. Asterisks indicate significant differences (*p < 0.05, **p < 0.01; two-tailed Student's t test) compared with the mock at the respective time point. The experiment was repeated with similar results.

(E) PR1 expression in Col and SMG7-ΔUTR-1 plants upon spray inoculation with virulent Pst DC3000. Expression values (mean ± SEM; averages of three biological replicates) are normalized to mock treatment.

(F) Bacterial titers of Pst DC3000 and Pst DC3000 hrcC⁻ in Col-0, two SMG7-ΔUTR lines, and eds1-2 mutants (mean ± SEM of five biological replicates; cfu = colony forming units). The experiment was repeated with similar results.

Asterisks in (B) and (F) indicate significant differences (*p < 0.05, **p < 0.01, ***p < 0.001; two-tailed Student's t test) compared to Col-0. See also Figures S6 and S7.

immune receptor transcripts. By so doing, NMD operates post-transcriptionally to control the threshold for activation of plant TNL and basal resistance pathways.

While smg7 autoimmunity relies genetically on key regulators of TNL and basal resistance, disruption of SA biosynthesis in smg7 sid2 mutants only mildly mitigated autoimmune symptoms (Figures 1A, 1B, S1A, and S1C). This fits with SA serving more as a defense signal amplifier in systemic tissues and often being dispensable for NLR local immunity (Fu and Dong, 2013; Tsuda et al., 2013). Although smg7 mutants displayed enhanced resistance to virulent Pst DC3000 and poorly virulent Pst DC3000 hrcC⁻ (Figure S1F), they had unaltered early PTI responses

(Figures S1D and S1E), suggesting that NMD-regulated TNLs contribute to EDS1/PAD4-regulated postinfection basal resistance pathways at a point downstream of early PTI mechanisms.

By exploring Arabidopsis natural variation, we found that NMD deficiency-conditioned autoimmunity can be elicited by a Ler allelic form of the TNL RPS6, reinforcing the link between NMD deficiency and TNL receptor actions. While RPS6 is causal for autoimmunity in the Ler accession (Figures 4A–4C), at least two other yet unidentified genetic loci underlie autoimmunity in Col plants. Similarly, suppression of autoimmunity was observed in a portion of smg7 F2 plants derived from a cross between Col and accession Ws (data not shown). Thus, autoimmunity caused

by NMD deficiency might be conditioned by different TNLs in different *Arabidopsis* accessions. This is supported by our transcriptome data showing that NMD affects a broad set of TNL transcripts. We therefore propose that one physiological role of NMD is to prevent inappropriate TNL activation and its adverse effects on growth and fitness.

In contrast to TNLs (Figures 2A–2E), CNLs do not appear to be regulated by NMD (Figures S2D and S2F), which is consistent with the lack of NMD-eliciting features in CNL transcripts (Table S2). Several TNLs have been reported to undergo alternative splicing, a process that is frequently coupled to NMD (Gassmann, 2008). TNL *RPS6* in accession RLD is alternatively spliced upon pathogen infection, producing transcripts that contain PTCs and potentially encode truncated TIR-only or TIR-NB domain proteins (Kim et al., 2009). We found that a subset of *RPS6* splice isoforms generated by the excision of a cryptic intron were upregulated by NMD impairment, whereas transcript variants containing PTCs resulting from an intron retention (IR) event were unaffected (Figure S2G). This fits with the observation that PTCs generated by IR events generally do not elicit NMD in plants due to nuclear retention of these transcripts (Göhring et al., 2014).

Studies of weak *Arabidopsis* NMD mutants showed that even a slight attenuation of NMD increases immunity against bacterial infection (Jeong et al., 2011; Rayson et al., 2012; Riehs-Kearnan et al., 2012). We find that NMD efficiency declines in response to pathogen infection, leading to stabilization of TNL mRNAs and elevated mRNA levels of the NMD components *SMG7* and *BARENTSZ1* (Figures 5A and 5B). Disruption of NMD autoregulation by expressing the *SMG7-ΔUTR* construct led to constitutive NMD activity (Figures 7B, S6D, and S6E), suggesting that SMG7 might be a rate-limiting factor in plant NMD. Notably, *SMG7-ΔUTR* plants failed to stabilize NMD-regulated TNL transcripts upon bacterial infection and were more susceptible to virulent bacteria (Figures 7D, 7F, and S6G). The level of disease susceptibility was comparable to that of *eds1-2* mutants, suggesting that infection-modulated NMD significantly potentiates antimicrobial defenses. *PR1* induction upon infection was unaltered in *SMG7-ΔUTR* plants compared to wild-type (Figures 7E and S6H), suggesting that NMD promotes an EDS1/PAD4-regulated SA-independent resistance mechanism (Bartsch et al., 2006).

Some virulent pathogen effectors target proteins involved in RNA metabolism as a host cell reprogramming infection strategy (Pumplin and Voinnet, 2013). Our data argue that NMD suppression is part of an intrinsic host defense program to bolster resistance against pathogen infection (Figures 6A, 6B, and S7D). While the precise molecular events underlying NMD suppression during infection have yet to be clarified, one mechanism might involve downregulation of NMD factors, as indicated by a study reporting downregulation of *UPF1* and *UPF3* during *Pst* DC3000 infection (Jeong et al., 2011). However, we were unable to confirm these findings (Figures S7A–S7C). Alternatively, NMD suppression might result from infection-induced translation inhibition. Infection of plants with *Pst* DC3000 inhibits host translation (Pajerowska-Mukhtar et al., 2012), and translation inhibition plays an important role in *Drosophila* and *Caenorhabditis elegans* innate immunity (Chakrabarti et al., 2012; McEwan et al., 2012). In mammals, a major pathway for stress-induced NMD suppression requires GCN2-mediated translational inhibition (Karam et al., 2013). However, we found that reduced NMD upon amino acid starvation or pathogen infection is independent of GCN2 in *Arabidopsis* (Figures S5A–S5D). Other translational regulators such as TOR, which has overlapping functions with GCN2 in yeast (Staschke et al., 2010), might be involved in infection-triggered NMD inhibition.

Plant NLRs are intracellular sensors of pathogen effector activities. However, there is evidence that NLRs also contribute to basal resistance mechanisms against virulent pathogens in the absence of recognizable ETI. For example, overexpression of the TNLs RPS4 and SNC1 elicits immune responses without effector triggering (Stokes et al., 2002; Wirthmueller et al., 2007). Thus, suppression of NMD leading to increases in NMD-controlled TNLs would be expected to boost basal resistance.

NLR expression requires exquisite control at multiple levels to prevent inappropriate activation of immune responses (Staiger et al., 2013). Transcriptional gene silencing through RNA-directed DNA methylation (RdDM), posttranscriptional gene silencing (PTGS) by different small RNA species, and alternative splicing all impose a constraint. Epigenetic control of NLR expression was demonstrated for the TNL *RMG1*, which is suppressed by RdDM (Yu et al., 2013). At a posttranscriptional level, microRNAs regulate the expression of numerous NLRs in *Medicago*, tobacco, tomato, and *Arabidopsis* (Boccara et al., 2014; Li et al., 2012; Shivaprasad et al., 2012; Zhai et al., 2011). Interference with PTGS by viral and bacterial suppressors can lead to derepression of PTGS-controlled NLRs and thus re-establishment of basal and NLR-conditioned immunity (Boccara et al., 2014; Shivaprasad et al., 2012). While PTGS appears to regulate both TNLs and CNLs, our analysis shows that NMD targets mainly TNLs (Figures 2B–2E, S2E, and S2G). Therefore, PTGS and NMD pathways might affect different NLR gene sets to modulate defense thresholds. Taken together, our findings emphasize the role of NMD in physiological processes and underscore the importance of RNA-based regulatory mechanisms in plant immunity.

EXPERIMENTAL PROCEDURES

Plant Materials and Growth Conditions

Wild-type *Arabidopsis thaliana* accessions used were Columbia-0 (Col) and Landsberg *erecta* (L*er*). Mutant and transgenic lines are described in the Supplemental Experimental Procedures. Plants were grown on soil with 16 hr light/8 hr dark photoperiod (21°C, 60% relative humidity), except for temperature shift experiments (28°C, 60% relative humidity) and experiments involving pathogen assays.

Pathogen Assays

Five-week-old soil-grown plants (8/16 hr photoperiod, 21°C) were spray inoculated with 1×10^8 cfu/ml *P. syringae pv tomato* DC3000 (*Pst* DC3000), or *Pst* DC3000 *hrcC⁻* with 0.04% (v/v) Silwet L-77 (Lehle Seeds), or 10 mM $MgCl_2$ as mock control, and bacterial titer was determined 72 hpi by serial dilution as previously described (Rietz et al., 2011). Samples for gene expression analysis were harvested from the same plant material. For comparison of NMD inhibition upon *Pst* DC3000 and *Pst* DC3000 *hrcC⁻* inoculation, leaves of 4- to 5-week-old Col plants (8/16 hr photoperiod, 21°C) were syringe infiltrated with 5×10^6 cfu/ml bacteria. For testing of HR outputs, leaves of 4- to 5-week-old plants were syringe infiltrated with 1×10^7 cfu/ml *Pst* DC3000 HopA1, and disease symptoms were recorded 24 hr after inoculation. Flg22 treatments of 12-day-old seedlings with 1 μM flg22 were performed as described by Tsuda et al. (2013). Alternatively, 1 μM flg22 was syringe infiltrated into

leaves of 4- to 5-week-old plants grown at 21°C with 8/16 hr photoperiod as described by Boccara et al. (2014). Flg22 peptide (Genscript) was a gift from Lionel Navarro.

Gene Expression Analysis

Total RNA was isolated from plant tissue using peqGOLD RNAPure (peqLab). Genomic DNA was removed from RNA samples using Ambion TURBO DNA-free (Life Technologies), and 1 μg of DNA-free RNA was reverse transcribed using the Maxima H Minus First Strand cDNA synthesis kit (Fermentas). One-fiftieth of cDNA was then amplified in qRT-PCR reactions using SsoAdvanced SYBR Green Supermix (Bio-Rad) and transcript-specific primers on a Bio-Rad iQ5 optical cycler. Expression was normalized to AT2G28390 or AT4G26410 (Czechowski et al., 2005) for steady-state levels and to eIF4A1 (AT3G13920) expression in transcriptional block experiments. All qRT-PCR data presented are from at least three biological replicates, each of which represents the average of three technical replicates. All primer sequences are listed in Table S3.

RNA-Seq Analysis

Single-end, strand-specific, and ribosomal RNA-depleted RNA-seq libraries were generated and sequenced using the ScriptSeq Complete Plant kit (Epicentre) on the Illumina HiSeq2000 platform. Experimental details are described in the Supplemental Experimental Procedures.

Transcriptional and Translational Inhibition

Transcriptional inhibition was performed in detached leaves of 4- to 5-week-old plants as previously described (Johnson et al., 2000) using a modified incubation buffer containing 1 mM PIPES (pH 6.25), 1 mM sodium citrate, 1 mM KCl, 15 mM sucrose, and 0.08% Silwet L-77. Leaves were soaked in incubation buffer for 30 min before the addition of cordycepin (150 μg/ml, Sigma). Vacuum was applied for 5 min and two leaves were then harvested after 1, 2, and 4 hr for subsequent RNA analysis. Transcript half-lives were calculated from qRT-PCR data by nonlinear least-square regression using GraphPad Prism 6.0. Translation inhibition was carried out for 5 hr using cycloheximide as previously described (Kalyna et al., 2012).

ACCESSION NUMBERS

The GEO accession number for the Illumina RNA-seq data set reported in this paper is GSE55884.

SUPPLEMENTAL INFORMATION

Supplemental Information includes Supplemental Experimental Procedures, seven figures, and four tables and can be found with this article online at http://dx.doi.org/10.1016/j.chom.2014.08.010.

AUTHOR CONTRIBUTIONS

J.G., J.E.P., and K.R. designed the experiments and wrote the manuscript. J.G., S.A., N.R., H.S., J.B., and B.D. performed experiments. A.S., B.K., and J.M.J.-G. performed computational analyses. J.G., C.J., H.S., N.R., J.E.P., and K.R. analyzed the data.

REFERENCES

Alcázar, R., and Parker, J.E. (2011). The impact of temperature on balancing immune responsiveness and growth in Arabidopsis. Trends Plant Sci. 16, 666–675.

Arciga-Reyes, L., Wootton, L., Kieffer, M., and Davies, B. (2006). UPF1 is required for nonsense-mediated mRNA decay (NMD) and RNAi in Arabidopsis. Plant J. 47, 480–489.

Ballut, L., Marchadier, B., Baguet, A., Tomasetto, C., Séraphin, B., and Le Hir, H. (2005). The exon junction core complex is locked onto RNA by inhibition of eIF4AIII ATPase activity. Nat. Struct. Mol. Biol. 12, 861–869.

Bartsch, M., Gobbato, E., Bednarek, P., Debey, S., Schultze, J.L., Bautor, J., and Parker, J.E. (2006). Salicylic acid-independent ENHANCED DISEASE SUSCEPTIBILITY1 signaling in Arabidopsis immunity and cell death is regulated by the monooxygenase FMO1 and the Nudix hydrolase NUDT7. Plant Cell 18, 1038–1051.

Boccara, M., Sarazin, A., Thiébeauld, O., Jay, F., Voinnet, O., Navarro, L., and Colot, V. (2014). The Arabidopsis miR472-RDR6 silencing pathway modulates PAMP- and effector-triggered immunity through the post-transcriptional control of disease resistance genes. PLoS Pathog. 10, e1003883.

Bruno, I.G., Karam, R., Huang, L., Bhardwaj, A., Lou, C.H., Shum, E.Y., Song, H.-W., Corbett, M.A., Gifford, W.D., Gecz, J., et al. (2011). Identification of a microRNA that activates gene expression by repressing nonsense-mediated RNA decay. Mol. Cell 42, 500–510.

Chakrabarti, S., Liehl, P., Buchon, N., and Lemaitre, B. (2012). Infection-induced host translational blockage inhibits immune responses and epithelial renewal in the Drosophila gut. Cell Host Microbe 12, 60–70.

Czechowski, T., Stitt, M., Altmann, T., Udvardi, M.K., and Scheible, W.-R. (2005). Genome-wide identification and testing of superior reference genes for transcript normalization in Arabidopsis. Plant Physiol. 139, 5–17.

Dodds, P.N., and Rathjen, J.P. (2010). Plant immunity: towards an integrated view of plant-pathogen interactions. Nat. Rev. Genet. 11, 539–548.

Drechsel, G., Kahles, A., Kesarwani, A.K., Stauffer, E., Behr, J., Drewe, P., Rätsch, G., and Wachter, A. (2013). Nonsense-mediated decay of alternative precursor mRNA splicing variants is a major determinant of the Arabidopsis steady state transcriptome. Plant Cell 25, 3726–3742.

Eberle, A.B., Lykke-Andersen, S., Mühlemann, O., and Jensen, T.H. (2009). SMG6 promotes endonucleolytic cleavage of nonsense mRNA in human cells. Nat. Struct. Mol. Biol. 16, 49–55.

Fu, Z.Q., and Dong, X. (2013). Systemic acquired resistance: turning local infection into global defense. Annu. Rev. Plant Biol. 64, 839–863.

Gardner, L.B. (2008). Hypoxic inhibition of nonsense-mediated RNA decay regulates gene expression and the integrated stress response. Mol. Cell. Biol. 28, 3729–3741.

Gassmann, W. (2005). Natural variation in the Arabidopsis response to the avirulence gene hopPsyA uncouples the hypersensitive response from disease resistance. Mol. Plant Microbe Interact. 18, 1054–1060.

Gassmann, W. (2008). Alternative splicing in plant defense. Curr. Top. Microbiol. Immunol. 326, 219–233.

Göhring, J., Jacak, J., and Barta, A. (2014). Imaging of endogenous messenger RNA splice variants in living cells reveals nuclear retention of transcripts inaccessible to nonsense-mediated decay in Arabidopsis. Plant Cell 26, 754–764.

Guo, Y.-L., Fitz, J., Schneeberger, K., Ossowski, S., Cao, J., and Weigel, D. (2011). Genome-wide comparison of nucleotide-binding site-leucine-rich repeat-encoding genes in Arabidopsis. Plant Physiol. 157, 757–769.

Heidrich, K., Wirthmueller, L., Tasset, C., Pouzet, C., Deslandes, L., and Parker, J.E. (2011). Arabidopsis EDS1 connects pathogen effector recognition to cell compartment-specific immune responses. Science 334, 1401–1404.

Heidrich, K., Blanvillain-Baufumé, S., and Parker, J.E. (2012). Molecular and spatial constraints on NB-LRR receptor signaling. Curr. Opin. Plant Biol. 15, 385–391.

Huang, L., Lou, C.-H., Chan, W., Shum, E.Y., Shao, A., Stone, E., Karam, R., Song, H.-W., and Wilkinson, M.F. (2011). RNA homeostasis governed by cell

type-specific and branched feedback loops acting on NMD. Mol. Cell *43*, 950–961.

Hwang, J., and Maquat, L.E. (2011). Nonsense-mediated mRNA decay (NMD) in animal embryogenesis: to die or not to die, that is the question. Curr. Opin. Genet. Dev. *21*, 422–430.

Isken, O., and Maquat, L.E. (2008). The multiple lives of NMD factors: balancing roles in gene and genome regulation. Nat. Rev. Genet. *9*, 699–712.

Jeong, H.-J., Kim, Y.J., Kim, S.H., Kim, Y.-H., Lee, I.-J., Kim, Y.K., and Shin, J.S. (2011). Nonsense-mediated mRNA decay factors, UPF1 and UPF3, contribute to plant defense. Plant Cell Physiol. *52*, 2147–2156.

Johnson, M.A., Perez-Amador, M.A., Lidder, P., and Green, P.J. (2000). Mutants of Arabidopsis defective in a sequence-specific mRNA degradation pathway. Proc. Natl. Acad. Sci. USA *97*, 13991–13996.

Jones, J.D.G., and Dangl, J.L. (2006). The plant immune system. Nature *444*, 323–329.

Kadota, Y., Shirasu, K., and Guerois, R. (2010). NLR sensors meet at the SGT1-HSP90 crossroad. Trends Biochem. Sci. *35*, 199–207.

Kalyna, M., Simpson, C.G., Syed, N.H., Lewandowska, D., Marquez, Y., Kusenda, B., Marshall, J., Fuller, J., Cardle, L., McNicol, J., et al. (2012). Alternative splicing and nonsense-mediated decay modulate expression of important regulatory genes in Arabidopsis. Nucleic Acids Res. *40*, 2454–2469.

Karam, R., Wengrod, J., Gardner, L.B., and Wilkinson, M.F. (2013). Regulation of nonsense-mediated mRNA decay: implications for physiology and disease. Biochim. Biophys. Acta *1829*, 624–633.

Kashima, I., Yamashita, A., Izumi, N., Kataoka, N., Morishita, R., Hoshino, S., Ohno, M., Dreyfuss, G., and Ohno, S. (2006). Binding of a novel SMG-1-Upf1-eRF1-eRF3 complex (SURF) to the exon junction complex triggers Upf1 phosphorylation and nonsense-mediated mRNA decay. Genes Dev. *20*, 355–367.

Kim, S.H., Kwon, S.I., Saha, D., Anyanwu, N.C., and Gassmann, W. (2009). Resistance to the Pseudomonas syringae effector HopA1 is governed by the TIR-NBS-LRR protein RPS6 and is enhanced by mutations in SRFR1. Plant Physiol. *150*, 1723–1732.

Kurihara, Y., Matsui, A., Hanada, K., Kawashima, M., Ishida, J., Morosawa, T., Tanaka, M., Kaminuma, E., Mochizuki, Y., Matsushima, A., et al. (2009). Genome-wide suppression of aberrant mRNA-like noncoding RNAs by NMD in Arabidopsis. Proc. Natl. Acad. Sci. USA *106*, 2453–2458.

Li, F., Pignatta, D., Bendix, C., Brunkard, J.O., Cohn, M.M., Tung, J., Sun, H., Kumar, P., and Baker, B. (2012). MicroRNA regulation of plant innate immune receptors. Proc. Natl. Acad. Sci. USA *109*, 1790–1795.

Maekawa, T., Kufer, T.A., and Schulze-Lefert, P. (2011). NLR functions in plant and animal immune systems: so far and yet so close. Nat. Immunol. *12*, 817–826.

McEwan, D.L., Kirienko, N.V., and Ausubel, F.M. (2012). Host translational inhibition by Pseudomonas aeruginosa Exotoxin A Triggers an immune response in Caenorhabditis elegans. Cell Host Microbe *11*, 364–374.

Mendell, J.T., Sharifi, N.A., Meyers, J.L., Martinez-Murillo, F., and Dietz, H.C. (2004). Nonsense surveillance regulates expression of diverse classes of mammalian transcripts and mutes genomic noise. Nat. Genet. *36*, 1073–1078.

Meyers, B.C., Kozik, A., Griego, A., Kuang, H., and Michelmore, R.W. (2003). Genome-wide analysis of NBS-LRR-encoding genes in Arabidopsis. Plant Cell *15*, 809–834.

Nyikó, T., Kerényi, F., Szabadkai, L., Benkovics, A.H., Major, P., Sonkoly, B., Mérai, Z., Barta, E., Niemiec, E., Kufel, J., and Silhavy, D. (2013). Plant nonsense-mediated mRNA decay is controlled by different autoregulatory circuits and can be induced by an EJC-like complex. Nucleic Acids Res. *41*, 6715–6728.

Okada-Katsuhata, Y., Yamashita, A., Kutsuzawa, K., Izumi, N., Hirahara, F., and Ohno, S. (2012). N- and C-terminal Upf1 phosphorylations create binding platforms for SMG-6 and SMG-5:SMG-7 during NMD. Nucleic Acids Res. *40*, 1251–1266.

Pajerowska-Mukhtar, K.M., Wang, W., Tada, Y., Oka, N., Tucker, C.L., Fonseca, J.P., and Dong, X. (2012). The HSF-like transcription factor TBF1 is a major molecular switch for plant growth-to-defense transition. Curr. Biol. *22*, 103–112.

Pumplin, N., and Voinnet, O. (2013). RNA silencing suppression by plant pathogens: defence, counter-defence and counter-counter-defence. Nat. Rev. Microbiol. *11*, 745–760.

Rayson, S., Arciga-Reyes, L., Wootton, L., De Torres Zabala, M., Truman, W., Graham, N., Grant, M., and Davies, B. (2012). A role for nonsense-mediated mRNA decay in plants: pathogen responses are induced in Arabidopsis thaliana NMD mutants. PLoS ONE *7*, e31917.

Riehs, N., Akimcheva, S., Puizina, J., Bulankova, P., Idol, R.A., Siroky, J., Schleiffer, A., Schweizer, D., Shippen, D.E., and Riha, K. (2008). Arabidopsis SMG7 protein is required for exit from meiosis. J. Cell Sci. *121*, 2208–2216.

Riehs-Kearnan, N., Gloggnitzer, J., Dekrout, B., Jonak, C., and Riha, K. (2012). Aberrant growth and lethality of Arabidopsis deficient in nonsense-mediated RNA decay factors is caused by autoimmune-like response. Nucleic Acids Res. *40*, 5615–5624.

Rietz, S., Stamm, A., Malonek, S., Wagner, S., Becker, D., Medina-Escobar, N., Vlot, A.C., Feys, B.J., Niefind, K., and Parker, J.E. (2011). Different roles of Enhanced Disease Susceptibility1 (EDS1) bound to and dissociated from Phytoalexin Deficient4 (PAD4) in Arabidopsis immunity. New Phytol. *191*, 107–119.

Schweingruber, C., Rufener, S.C., Zünd, D., Yamashita, A., and Mühlemann, O. (2013). Nonsense-mediated mRNA decay - mechanisms of substrate mRNA recognition and degradation in mammalian cells. Biochim. Biophys. Acta *1829*, 612–623.

Shivaprasad, P.V., Chen, H.-M., Patel, K., Bond, D.M., Santos, B.A.C.M., and Baulcombe, D.C. (2012). A microRNA superfamily regulates nucleotide binding site-leucine-rich repeats and other mRNAs. Plant Cell *24*, 859–874.

Staiger, D., Korneli, C., Lummer, M., and Navarro, L. (2013). Emerging role for RNA-based regulation in plant immunity. New Phytol. *197*, 394–404.

Staschke, K.A., Dey, S., Zaborske, J.M., Palam, L.R., McClintick, J.N., Pan, T., Edenberg, H.J., and Wek, R.C. (2010). Integration of general amino acid control and target of rapamycin (TOR) regulatory pathways in nitrogen assimilation in yeast. J. Biol. Chem. *285*, 16893–16911.

Stokes, T.L., Kunkel, B.N., and Richards, E.J. (2002). Epigenetic variation in Arabidopsis disease resistance. Genes Dev. *16*, 171–182.

Tan, X., Meyers, B.C., Kozik, A., West, M.A.L., Morgante, M., St Clair, D.A., Bent, A.F., and Michelmore, R.W. (2007). Global expression analysis of nucleotide binding site-leucine rich repeat-encoding and related genes in Arabidopsis. BMC Plant Biol. *7*, 56.

Trcek, T., Sato, H., Singer, R.H., and Maquat, L.E. (2013). Temporal and spatial characterization of nonsense-mediated mRNA decay. Genes Dev. *27*, 541–551.

Tsuda, K., Mine, A., Bethke, G., Igarashi, D., Botanga, C.J., Tsuda, Y., Glazebrook, J., Sato, M., and Katagiri, F. (2013). Dual regulation of gene expression mediated by extended MAPK activation and salicylic acid contributes to robust innate immunity in Arabidopsis thaliana. PLoS Genet. *9*, e1004015.

Unterholzner, L., and Izaurralde, E. (2004). SMG7 acts as a molecular link between mRNA surveillance and mRNA decay. Mol. Cell *16*, 587–596.

Wagner, S., Stuttmann, J., Rietz, S., Guerois, R., Brunstein, E., Bautor, J., Niefind, K., and Parker, J.E. (2013). Structural basis for signaling by exclusive EDS1 heteromeric complexes with SAG101 or PAD4 in plant innate immunity. Cell Host Microbe *14*, 619–630.

Weischenfeldt, J., Damgaard, I., Bryder, D., Theilgaard-Mönch, K., Thoren, L.A., Nielsen, F.C., Jacobsen, S.E.W., Nerlov, C., and Porse, B.T. (2008). NMD is essential for hematopoietic stem and progenitor cells and for eliminating by-products of programmed DNA rearrangements. Genes Dev. *22*, 1381–1396.

Wirthmueller, L., Zhang, Y., Jones, J.D.G., and Parker, J.E. (2007). Nuclear accumulation of the Arabidopsis immune receptor RPS4 is necessary for triggering EDS1-dependent defense. Curr. Biol. *17*, 2023–2029.

Yepiskoposyan, H., Aeschimann, F., Nilsson, D., Okoniewski, M., and Mühlemann, O. (2011). Autoregulation of the nonsense-mediated mRNA decay pathway in human cells. RNA *17*, 2108–2118.

Yoine, M., Nishii, T., and Nakamura, K. (2006). Arabidopsis UPF1 RNA helicase for nonsense-mediated mRNA decay is involved in seed size control and is essential for growth. Plant Cell Physiol. *47*, 572–580.

Yu, A., Lepère, G., Jay, F., Wang, J., Bapaume, L., Wang, Y., Abraham, A.-L., Penterman, J., Fischer, R.L., Voinnet, O., and Navarro, L. (2013). Dynamics and biological relevance of DNA demethylation in Arabidopsis antibacterial defense. Proc. Natl. Acad. Sci. USA *110*, 2389–2394.

Zhai, J., Jeong, D.-H., De Paoli, E., Park, S., Rosen, B.D., Li, Y., González, A.J., Yan, Z., Kitto, S.L., Grusak, M.A., et al. (2011). MicroRNAs as master regulators of the plant NB-LRR defense gene family via the production of phased, trans-acting siRNAs. Genes Dev. *25*, 2540–2553.

Supplemental Information

Nonsense-Mediated mRNA Decay Modulates Immune Receptor Levels to Regulate Plant Antibacterial Defense

Jiradet Gloggnitzer, Svetlana Akimcheva, Arunkumar Srinivasan, Branislav Kusenda, Nina Riehs, Hansjörg Stampfl, Jaqueline Bautor, Bettina Dekrout, Claudia Jonak, José M. Jiménez-Gómez, Jane E. Parker, Karel Riha

Supplemental Figures

Figure S1
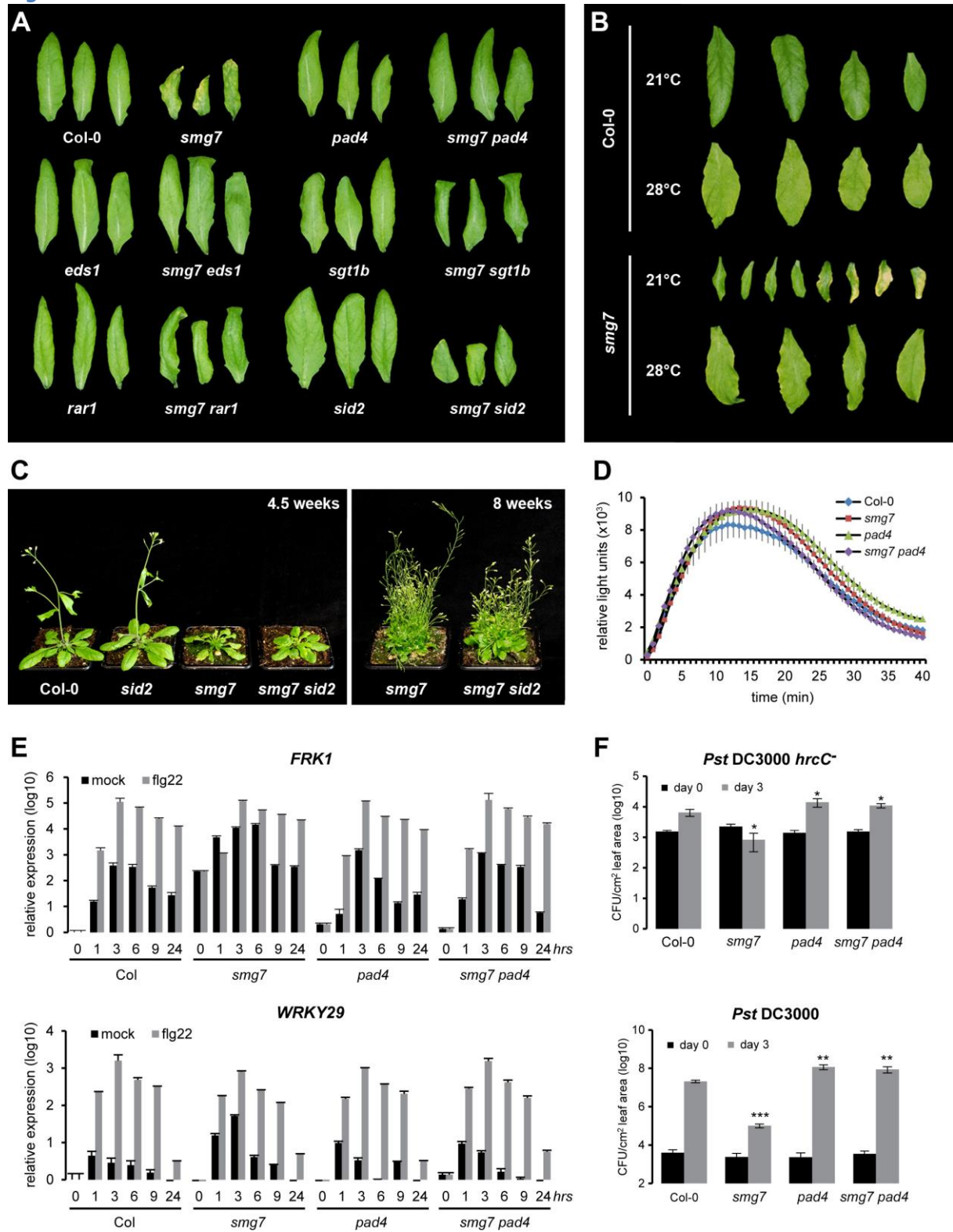
Figure S1, Related to Figure 1. Genetic and environmental requirements for immune response activation in *smg7* mutants

(A) Detached leaves of five-week old plants of the indicated genotypes.

(B) Detached leaves of five-week old Col-0 and *smg7* plants grown at 21°C and 28°C.

(C) Shown are 4.5-week old Col-0, *smg7*, *sid2* and *smg7 sid2* plants. The *sid2* mutation failed to suppress stunting of *smg7* single mutants. The *smg7* and *smg7 sid2* plants shown in the left panel were propagated for a total of 8 weeks and are shown in the right panel.

(D) ROS burst dynamics measured in leaf discs of 5-week-old plants of Col-0, *smg7*, *pad4*, and *smg7 pad4* plants in response to 100 nM flg22. Results are mean ±SD (n=16).

(E) Expression dynamics of PTI marker genes *FRK1* and *WRKY29* in Col-0, *smg7*, *pad4*, and *smg7 pad4* plants upon syringe infiltration plants of 1 µM flg22 or water (mock) into leaves of 5 week-old plants. Average values (±SEM, three replicates) are shown and are normalized to mRNA levels in Col plants at 0h.

(F) Bacterial titers of Col-0, *smg7*, *pad4*, and *smg7 pad4* plants after spray inoculation with *Pst* DC3000 and *Pst* DC3000 *hrcC⁻* at day 0 and day 3 post-inoculation. Values (±SEM) represent the average of five biological replicates. Asterisks indicate significant differences (*$p<0.05$, **$p<0.01$, ***$p<0.001$; two-tailed Student's t-test).

Figure S2
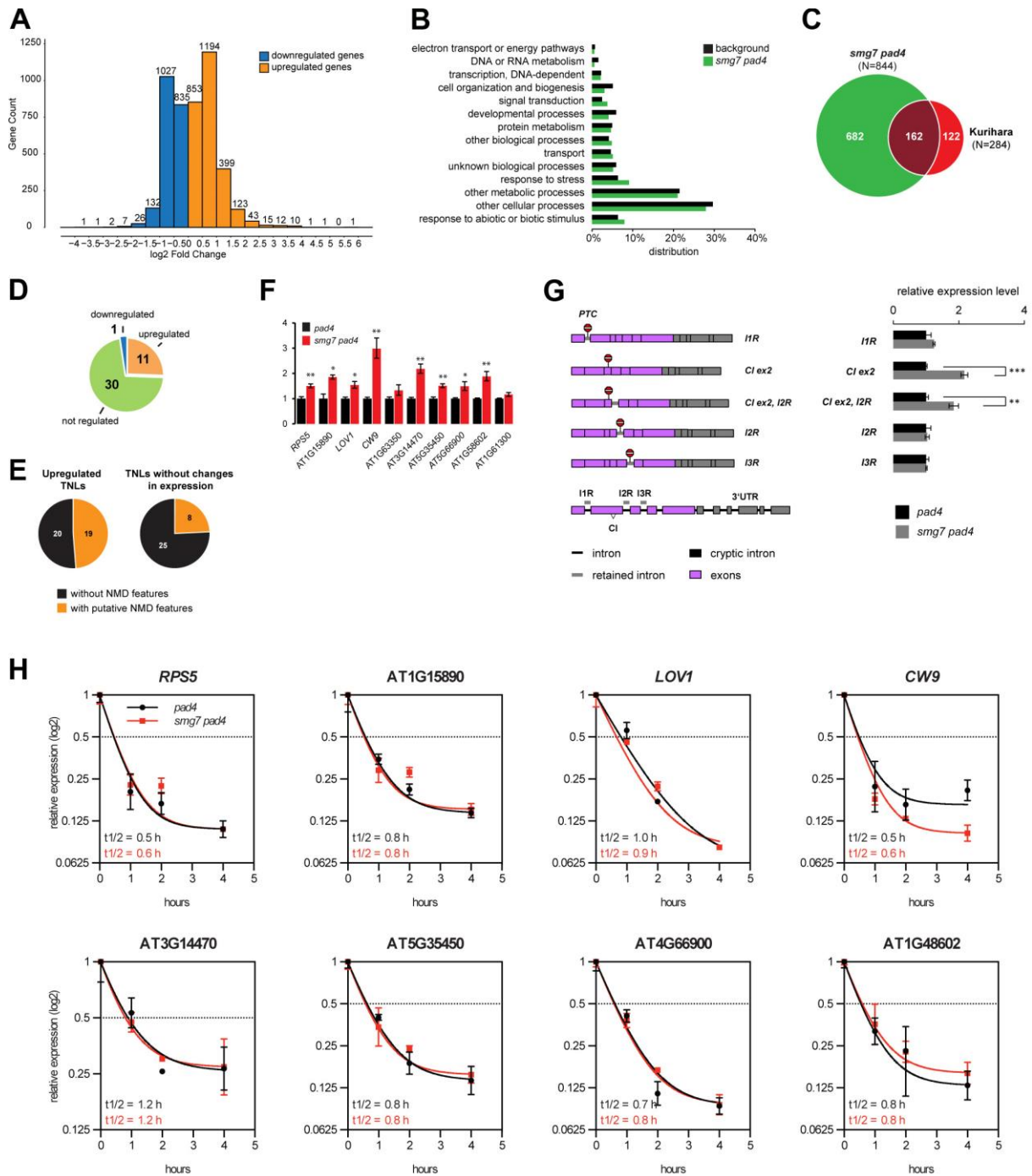
Figure S2, Related to Figure 2. RNA-seq analysis of *smg7 pad4* mutants

(A) Histogram showing the fold-change (log2) distribution of significantly up- and downregulated transcripts in *smg7 pad4* mutant relative to *pad4* control plants (adjusted *p*-value *q*<0.05). Numbers on the bars indicate numbers of transcript in the respective fold-change range indicated on the x-axis.

(B) Distribution of functional gene ontology (GO) terms of transcripts that are significantly upregulated in *smg7 pad4* mutants (green bars) (adjusted *p*-value *q*<0.05), compared to GO terms present in the background set (black bars).

(C) Proportional Venn diagram illustrating the overlap of 284 genes that were found to be upregulated (fold change >1.8) in the NMD mutants *upf1-1* and *upf3-1* by Kurihara et al., (2009) and 844 genes that were significantly upregulated (fold change 1.8, *q*<0.05) in *smg7 pad4* RNA-seq data sets. The two data sets have 162 genes in common, while 122 genes are uniquely present in the Kurihara data set and 682 genes are only present in the *smg7 pad4* set.

(D) Classification of significantly upregulated or downregulated (*q*<0.05) and expressed but not significantly changed CNL transcripts (*q*≥0.05) in *smg7 pad4* relative to *pad4* plants. The number of transcripts in each category is indicated.

(E) Pie-charts showing the distribution of putative NMD eliciting features among expressed TNL genes that were either found to be upregulated in *smg7 pad4* mutants (left) or that were not subjected to differential regulation (right).

(F) Steady state levels of selected CNL transcripts in *pad4* and *smg7 pad4* measured by qRT-PCR. Average values (±SEM) of three biological replicates are shown. Asterisks indicate significant differences (*$*p$<0.05, **p<0.01, ***p<0.001) compared to *pad4* control samples (two-tailed Student's t-test).

(G) qRT-PCR-based quantification of *RPS6* splice variants. Asterisks (*) indicate statistically significant differences determined by Student's test (two-tailed, **p<0.01, ***p<0.001). Values are averages of three biological replicates and are normalized to the expression of AT2G28390. Error bars denote standard error of mean (SEM). A scheme of previously reported *RPS6* splice variants is depicted on the left (Kim et al., 2009) and was adapted from Staiger and Brown (2013). I1R=intron 1 retention, I2R = intron 2 retention, I3R=intron 3 retention, CI ex2= excision of a cryptic intron located in exon 2.
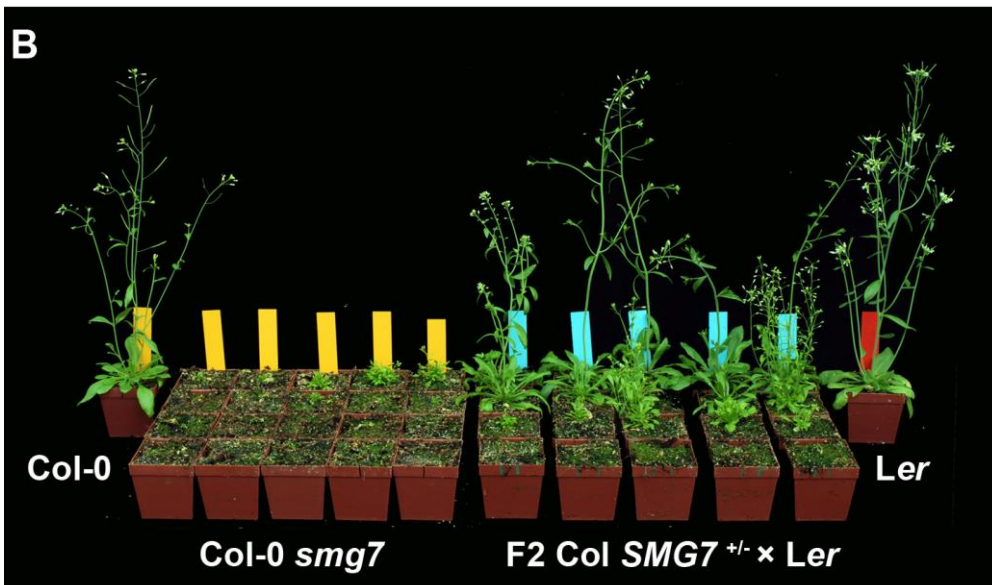
(G) qRT-PCR analysis of mRNA half-lives of CNL transcripts. Transcription was inhibited in *pad4* and *smg7 pad4* plants and half-lives ($t_{1/2}$) were calculated by non-linear least square regression. Average values (±SEM) of three biological replicates are shown (normalized to *eIF4A1* expression). The experiment was repeated twice with similar results.

A
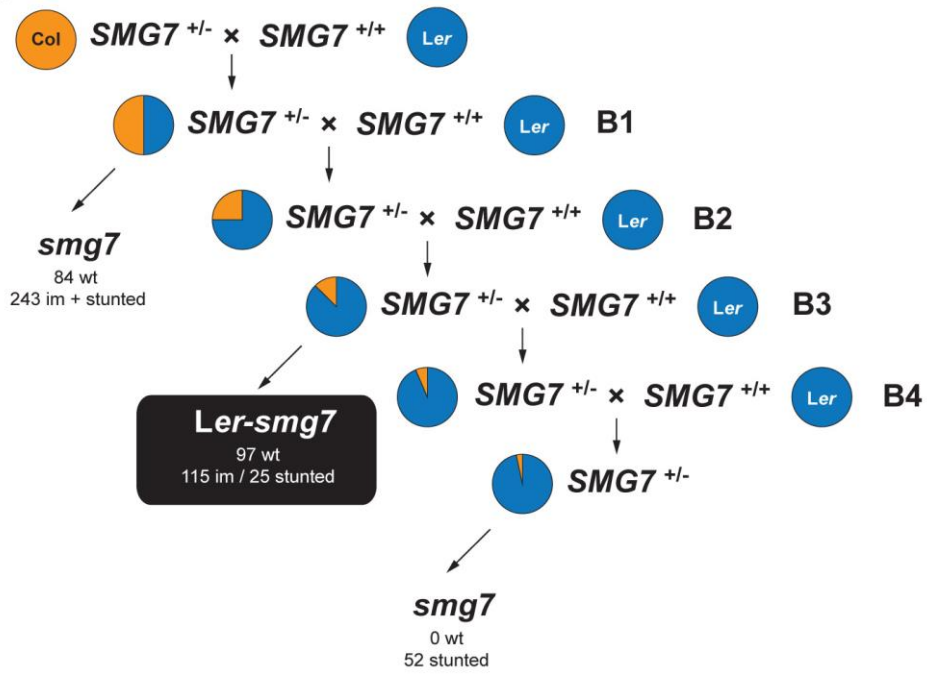
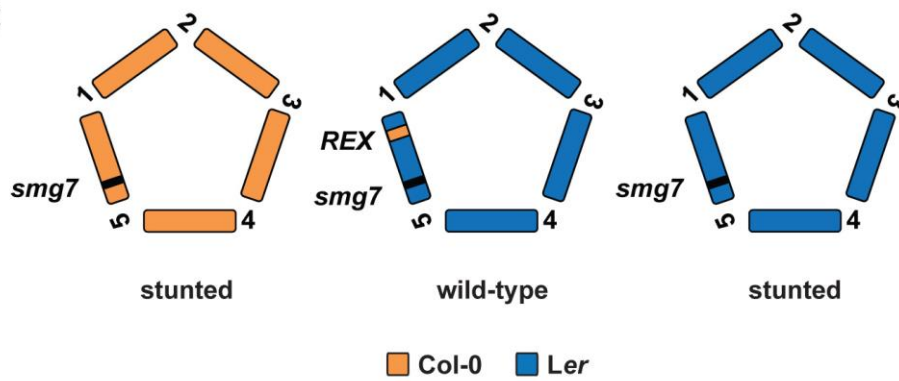**B**

C

Figure S3, Related to Figure 3. Map-based cloning of *REX*

(A) A crossing scheme delineating the crosses performed for map-based cloning of *REX/RPS6.* Progeny of the first cross, and second and fourth backcrosses (B2 and B4) were allowed to self and *smg7* mutants were phenotypically analyzed. Numbers below indicate the number of *smg7* plants that were stunted, had wild-type (wt) appearance or showed an intermediate (im) phenotype. A range of intermediate to stunted phenotypes was detected in the F2 population derived from the first cross to L*er* (im + stunted). The population highlighted by a black box (L*er-smg7*) was used to fine-map *REX*.

(B) Plants shown are mutant *smg7* F2 progeny from a cross of *SMG7*$^{+/-}$ plants (Col background) to L*er* wild-type plants. In this F2 population suppression of stunting was observed in 84 plants, while 243 remained stunted or had an intermediate phenotype (see also Figure S3A).

(C) Illustration of genotypes that were obtained in map-based cloning of the *REX* locus. The *smg7* mutation was generated in the Col accession (left panel) and is located on chromosome 5. Col-*smg7* mutants are stunted and suffer from autoimmunity. Introgression of the *smg7* mutation into L*er* genomic background by multiple backcrosses yields plants that are also stunted (right panel). However, *smg7* mutants in Ler background (L*er-smg7*) that retain Col genome on the right arm of chromosome 5 (*REX* locus) have wild-type appearance and show no disease symptoms (middle panel).
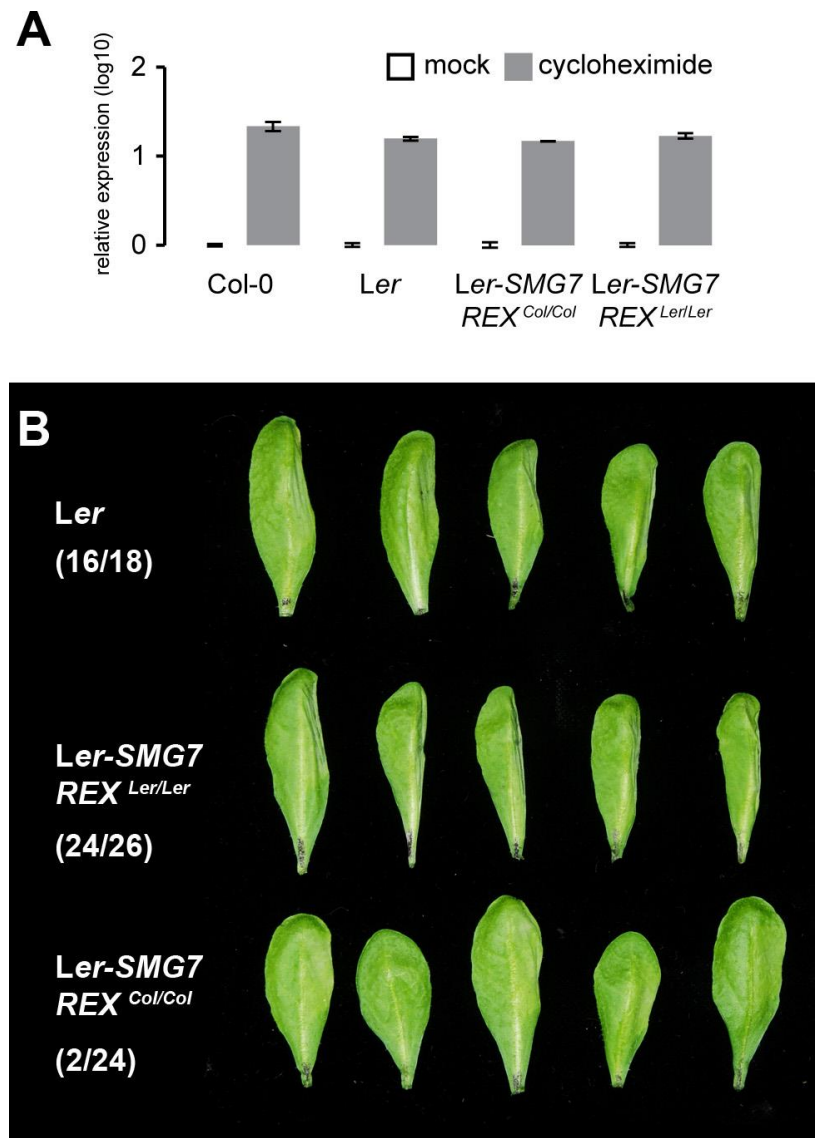
Figure S4, Related to Figure 4. Col and *Ler* alleles of *RPS6* are NMD targets and trigger different HR outputs.

(A) Expression levels of *RPS6* upon translational inhibition with cycloheximide in 14-day old seedlings of the indicated genotypes. Expression levels shown are averages of four biological replicates (±SEM). Values are normalized to the expression of AT2G28390.

(B) Syringe infiltration into the right side of leaves of the indicated genotypes with 1×10^7 cfu/mL *Pst* DC3000 HopA1. HR symptoms were recorded 24 hours after infiltration. L*er*-*SMG7* plants with the *REX^Ler^* allele display tissue collapse in the infiltrated region, while this is not the case in L*er*-*SMG7* plants carrying the *REX^Col^* allele. Numbers in parenthesis indicate the number of leaves displaying tissue collapse vs. total number of infiltrated leaves.
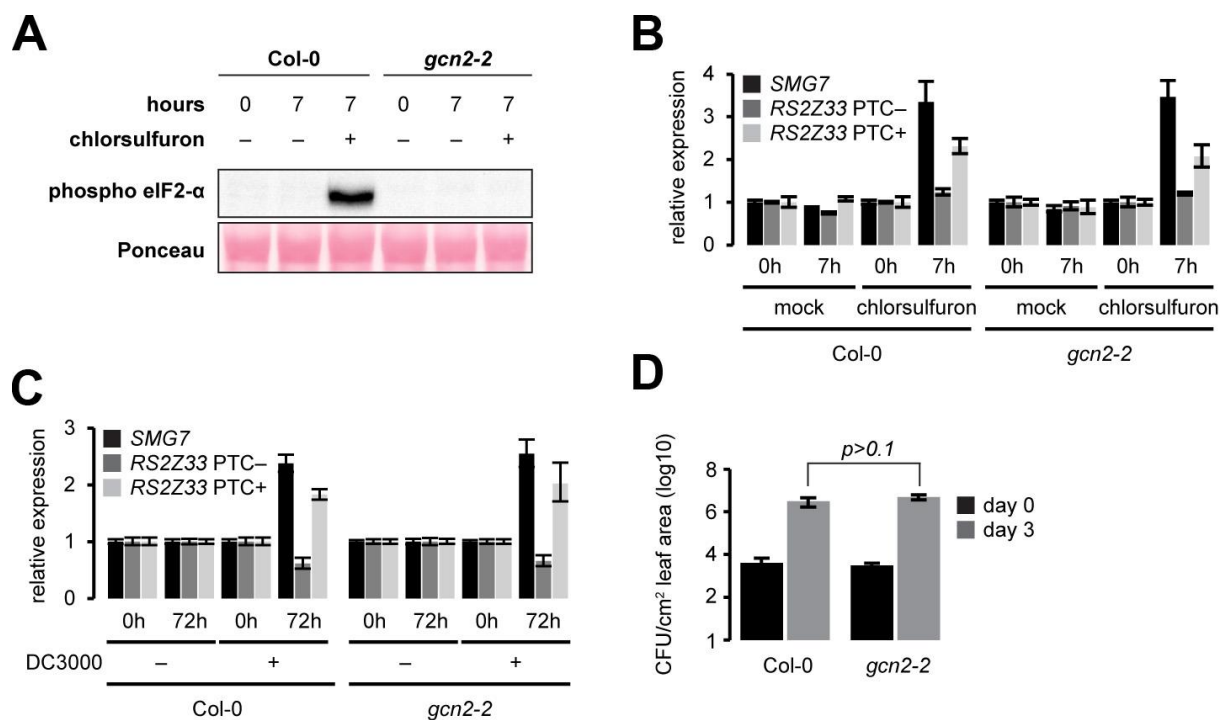
Figure S5, Related to Figure 5. The eIF2α-kinase GCN2 is dispensable for NMD downregulation in response to amino acid starvation and pathogen infection

(A) Western Blot analysis of 12-day old Col wild-type seedlings and *gcn2-2* mutant seedlings. To induce amino acid starvation, the seedlings were treated for 7 hours with 0.6 μM chlorsulfuron, an inhibitor of amino acid biosynthesis, as described by Lageix et al. (2008). Phosphorylation of eIF2α is readily detected in Col seedlings after chlorsulfuron treatment, while no phosphorylation is detected in *gcn2-2* seedlings, confirming loss of function of GCN2 in *gcn2-2* mutants. Similar results were obtained with another *gcn2* mutant line in L*er* background (Genetrap line GT8359, Cold Spring Harbor Laboratory) (data not shown). Ponceau staining of Rubisco large subunit (rbcL) is shown as a loading control.

(B) Expression levels of *SMG7* and PTC-/+ splice variants of *RS2Z33* measured by qRT-PCR in Col and *gcn2-2* seedlings upon amino acid starvation induced by chlorsulfuron. Expression levels shown are averages of four biological replicates (±SEM). Values are normalized to the expression of AT2G28390. The *SMG7* and *RS2Z33* PTC+ mRNAs are specifically upregulated in response to chlorsulfuron treatment in both Col and *gcn2-2* seedlings, indicating that NMD downregulation occurs independently of the presence of a functional *GCN2* allele. Similar results were obtained Genetrap Line GT8359. The experiment was repeated with similar results.

(C) Expression levels of *SMG7* and PTC-/+ splice variants of *RS2Z33* measured by qRT-PCR in Col and *gcn2-2* plants at day 0 and 3 days later after spray inoculation with *Pst* DC3000 (1x10^8 cfu/ml). Values (±SEM) represent the average of three biological replicates. Accumulation of *SMG7* and *RS2Z33* PTC+ was observed in *Pst* DC3000 treated Col and *gcn2-*

2, indicating that NMD downregulation upon *Pst* DC3000 treatment occurs independently of GCN2.

(D) Bacterial growth assay in Col wild-type plants and *gcn2-2* mutant plants at day 0 and 3 days later after spray inoculation with *Pst* DC3000 ($1x10^8$ cfu/ml). Values (±SEM) represent the average of five biological replicates (each consisting of 4 leaves per plant). Bacterial growth is not significantly different between infected Col and *gcn2-2* mutants ($p>0.1$, two-tailed Student's t-test). These data suggest that GCN2 kinase is dispensable for basal resistance against virulent *Pst* DC3000.

Figure S6
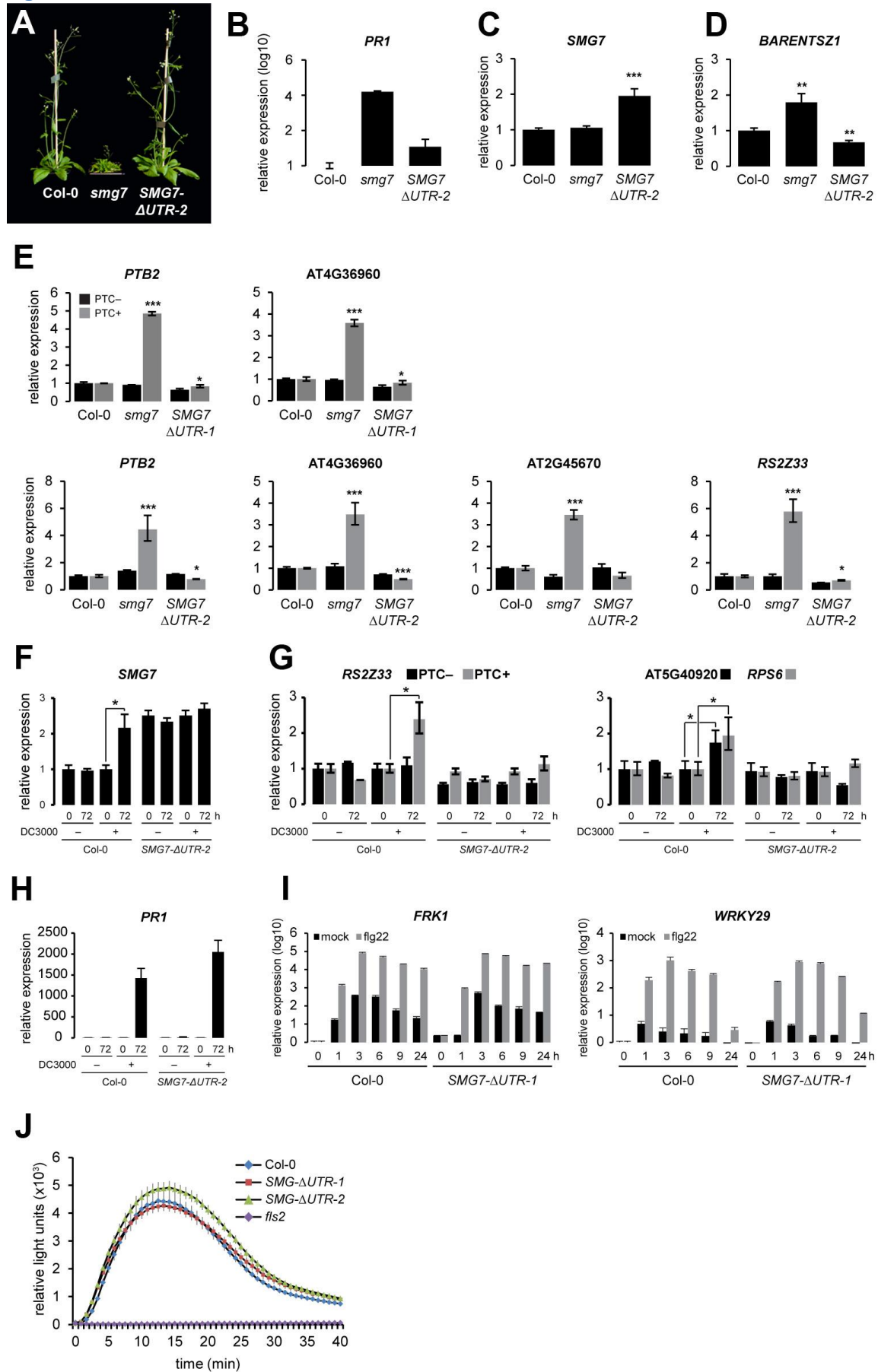
Figure S6, Related to Figure 7. Impairment of NMD autoregulation reduces basal resistance

(A) Five week old Col wild-type, *smg7* and an independent transgenic *smg7* mutant line complemented with *SMG7* cDNA lacking the endogenous 3'UTR (*SMG7-ΔUTR-2*) are shown.

(B-D) Expression of *PR1* and NMD components *SMG7* and *BARENTSZ1* measured by qRT-PCR in Col-0, smg7, and *SMG7-ΔUTR-2* plants. Values for *SMG7* in *SMG7-ΔUTR-2*plants are total mRNA levels of endogenous *SMG7* and the *SMG7* cDNA transgene. Values are averages of four biological replicates (±SEM). Statistical significance in (C) and (D) was tested with a two-tailed Student's t-test. Asterisks indicate significant differences (**$p<0.01$, ***$p<0.001$).

(E) Expression of NMD reporters measured by qRT-PCR in wild-type, *SMG7-ΔUTR-1 and SMG7-ΔUTR-2.* Values are averages of four biological replicates (±SEM). Asterisks indicate significant differences (*$p<0.05$, **$p<0.01$; two-tailed Student's t-test).

(F-G) Expression of *SMG7*, the NMD reporter *RS2Z33* and TNL*s RPS6* and AT5G40920 measured by qRT-PCR in wild-type and *SMG7-ΔUTR-1* plants after spray-inoculation with virulent *Pst* DC3000 (+) or mock inoculation (-) with MgCl$_2$. Values are averages of three biological replicates (±SEM) and are relative to Col steady state levels at 0 hpi. Asterisks indicate significant differences (*$p<0.05$; two-tailed Student's t-test) compared with the mock control at the respective time point (two-tailed Student's t-test).

(H) *PR1* expression measured by qRT-PCR in Col-0 and *SMG7-ΔUTR-1 plants* upon spray-inoculation with virulent *Pst* DC3000 (+) or MgCl$_2$ (-). Expression values (±SEM; averages of three biological replicates) are normalized to mock treatment.

(I) Expression dynamics of PTI marker genes *FRK1* and *WRKY29* in Col, *smg7*, *SMG7-ΔUTR-1*, and *SMG7-ΔUTR-2* plants upon syringe infiltration of 1 µM flg22 or water (mock) into leaves of 5 week-old plants. Average values (±SEM, three replicates) are shown and are normalized to mRNA levels in Col plants at 0h.

(J) ROS burst dynamics measured in leaf discs of 5-week-old plants of Col, *smg7*, *SMG7-ΔUTR-1*, and *SMG7-ΔUTR-2* in response to 100 nM flg22. Results are mean ±SD (n=17).
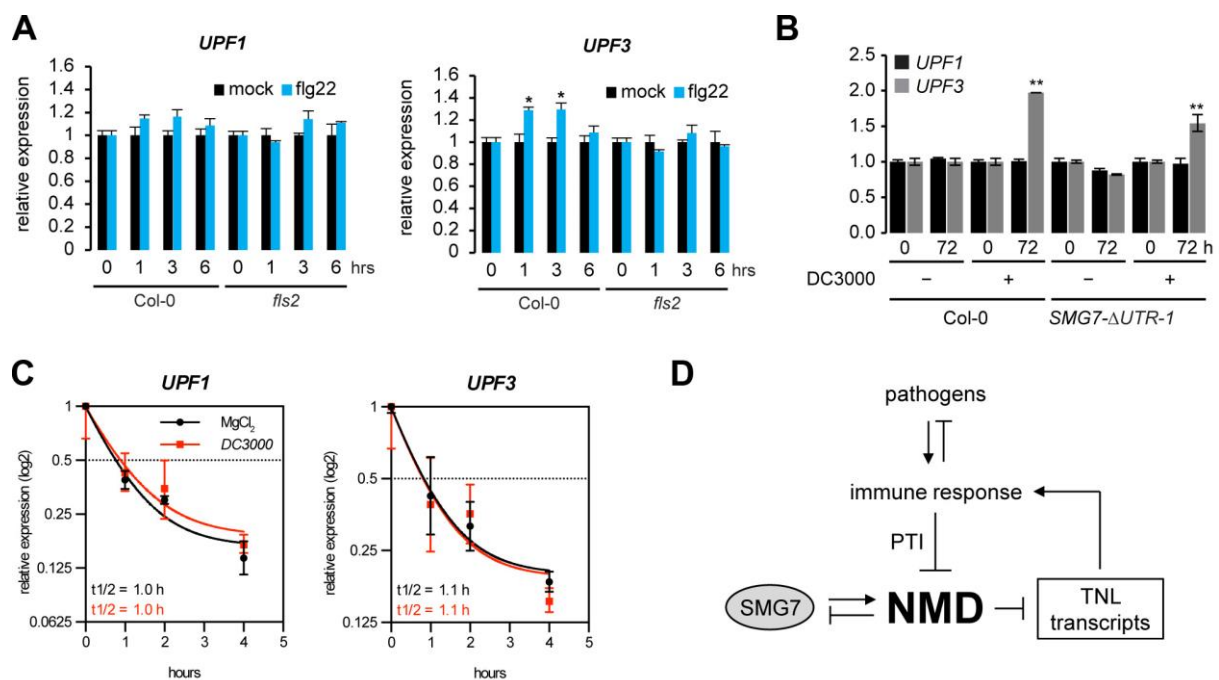
Figure S7, Related to Figure 7. Expression levels and mRNA stability analysis of NMD factor transcripts *UPF1* and *UPF3*.

(A) Expression of *UPF1* and *UPF3* measured by qRT-PCR upon flg22 treatment (1 μM) of seedlings (average values ±SEM of three biological replicates). The expression of *UPF1* remains unaltered in response to flg22, while *UPF3* mRNA is induced at 1 and 3 hours in flg22 treated Col-0 wild-type seedlings. *UPF3* upregulation is abolished in the *fls2* mutant. Expression values were normalized to mock treatment at the respective time point and asterisks indicate significant differences (*p<0.05) to mock (two-tailed Student's t-test). The experiments were repeated with similar results.

(B) Expression of *UPF1 and UPF3* measured by qRT-PCR in wild-type and *SMG7-ΔUTR-1* plants after spray-inoculation with virulent *Pst* DC3000 (+) or mock inoculation with MgCl$_2$ (-). Values are averages of three biological replicates (±SEM) and are relative to Col-0 steady state levels at 0 hpi. Asterisks indicate significant differences (**p<0.01; two-tailed Student's t-test) compared with the mock control at the respective time point. In both wild-type and *SMG7-ΔUTR-1* plants, *UPF1* transcript levels remain unaffected after *Pst* DC3000 treatment, while *UPF3* levels significantly increase when compared to mock, suggesting that *UPF1* and *UPF3* transcript levels do not account for constitutive NMD activity and reduced basal resistance in *SMG7-ΔUTR-1* plants.

(C) qRT-PCR analysis of half-lives of *UPF1* and *UPF3* after pathogen infection (see also Figure 5B). Transcription was inhibited in wild-type plants 72 h after mock treatment or treatment with *Pst* DC3000. *UPF1* and *UPF3* transcript stability remains unaffected upon *Pst* DC3000 inoculation, suggesting that both transcripts are not regulated through NMD. Transcript half-

lives ($t_{1/2}$) were calculated by non-linear least square regression. Average values (±SEM) of three biological replicates are shown (normalized to *eIF4A1* expression). The experiment was repeated three times with similar results.

(D) Model depicting the role of NMD in plant innate immunity.

Table S3, Related to Experimental Procedures. Primers used in this study

PCR-genotyping of mutants

Name	Sequence (5'→3')	Remarks
Est1b-1	GACCTTGGTAGCTGGTCC TGAG	PCR genotyping of *smg7-1* and SMG7 cDNA wt: Est1b-1 + Est1b-2 mut: Est1b-1 + LBc-1
Est1b-2	GGACAACAGGCCAACCATTCAAC	
LBc-1	TGGACCGCTTGCTGCAACTCT	
pad4-1-F	GCGATGCATCAGAAGAG	PCR genotyping of *pad4-1* CAPS marker (BsmF1)
pad4-1-R	TTAGCCCAAAAGCAAGTATC	
105/E2	ACACAAGGGTGATGCGAGACA	PCR genotyping of *eds1-2*, multiplex PCR Wt: 1500 bp + 750 bp Mut: 1500 bp + 600 np
EDS4	GGCTTGTATTCATCTTCTATCC	
EDS6	GTGGAAACCAAATTTGACATTAG	
sgt1b-F dc_eta3_AluI-F	AGGATGAGAAGCTTGATGGAGATGCACC	PCR genotyping of *sgt1b (eta3),* CAPS marker (AluI)
sgt1b-F dc_eta3_AluI-R	CGTCCCATTCGACTCTGCCTGTCAAAGC	
rar1-21-F PM100	AACTTTTGCCACCGGTTATG	PCR genotyping of *rar1-21* CAPS marker (Cac8I)
rar1-21-R PM101	GGCCAGAACTGGTTTCTCAG	
SID2-F2	GCTCTGCAGCTTCAATGC	PCR genotyping of *sid2-1* CAPS marker (TruI1)
SID2-R2	CGAAGAAATGAAGAGCTTGG	

Primer for quantitative real-time PCR (qRT-PCR)

Name	Sequence (5'→3')	Remarks
PR1-qF2	GCTCTTGTAGGTGCTCTTGTTCTTCC	qRT-PCR for AT2G14610 (*PR1*)
PR1-qR2	AGTCTGCAGTTGCCTCTTAGTTGTTC	
NMD3-PTC-qF2	TACGGAAGAGTGCGAGATGTGG	qRT-PCR for AT2G37340 (*RS2Z33*) PTC– splice variant
NMD3-PTC-qR2	GGGATCACCAAATTCAACGAAAGC	
NMD3+PTC-qF2	CGCCTTGGCGATTCTGTTTGTAG	qRT-PCR for AT2G37340 (*RS2Z33*) PTC+ splice variant
NMD3+PTC-qR2	GGGATCACCAAATTCAACGAAAGC	
NMD2-PTC-qF2	TGCTGTGCATGAAATAAAGAGAAAA	qRT-PCR for AT2G45670 PTC– splice variant
NMD2-PTC-qR2	TCGTGGTTCCTTCGGGGAAT	
NMD2+PTC-qF2	TGCTGTGCATGAAATAAAGGGATGT	qRT-PCR for AT2G45670 PTC+ splice variant
NMD2+PTC-qR2	AGTCGTGGTTCCTTCGGGGA	
AT1G31540-qF1	GAAGCGCATGCGGCTATATCAC	qRT-PCR for AT1G31540
AT1G31540-qR1	CCGTTTAGTTTGGACGTAGACACC	
AT1G72840-qF1	GGCAAGCATTCCAGAAATTGCG	qRT-PCR for AT1G72840
AT1G72840-qR1	CTTGGCAGTCGACTTGAGATGC	
AT1G72940-qF1	GACGAGCATTGACCAGTTTGGC	qRT-PCR for AT1G72940
AT1G72940-qR1	GCTTCGCTTCATCTTCACATTGG	
AT4G12020-qF1	GGGTAACAACAGGTGATGCCTTG	qRT-PCR for AT4G12020
AT4G12020-qR1	TGACGCCACTAGTGTCAACTCC	
AT5G41740-qF1	TGAAGCAGAAGGTTCCAAGTTCTC	qRT-PCR for AT5G41740
AT5G41740-qR1	TCTTCTTCACTGACCAAGCTTCCG	
AT5G51630-qF1	TGGGATGTCTCTCCCAGAGTTC	qRT-PCR for AT5G51630
AT5G51630-qR1	AGCTTCACCTTCACCTTTAACTGG	
AT5G40920-qF2	GTTGGCAAATGAAACAGGTACTGG	qRT-PCR for AT5G40920
AT5G40920-qR2	GCATCCCTTCAAAGACTCGTTTCC	
RPS6-3UTR-qF2	ACCAAAGCATGGATCTCCCGGTC	qRT-PCR for AT5G46470 (*RPS6*),

RPS6-3'UTR-qR2	CGCACAGAGCTCTTCTCCACTGA	amplifies Col and L*er* alleles
RPS6-B-qF2	TGGTTGTGAAATGGTCTGTTTCCTT	qRT-PCR for RPS6-I1R
RPS6-B-qR2	TCCCGACCATCCTCACTTCCTC	
RPS6-C-qF1	ATGTATTTTCAATGAGATCCCTTATC	qRT-PCR for RPS6-CI ex2
RPS6-C-qR1	CCTTCTTAGTACCAGTGTTATGTTCAA	
RPS6-D-qF2	TGTATTTTCAATGAGATCCCTTATCTGT	qRT-PCR for RPS6-CI ex2, I2R
RPS6-D-qR2	ACAATTCTGCACATATGAAATGACATGC	
RPS6-I2R-qF2	TCGGGCTAAAAAACCTTGTTGATAG	qRT-PCR for RPS6-I2R
RPS6-I2R-qR2	ACCAATTCGTTACAATTCTGCACAT	
RPS6-I3R-qF1	TCTACCAGGATTAATATCGACATTGGAA	qRT-PCR for RPS6-I3R
RPS6-I3R-qR1	CCCTGCAAGTGACTGAATTATATGCAA	
AT5G46490 -qF1	TCTACCGAATGGAATCGCGGA	qRT-PCR for AT5G46490
AT5G46490-qR1	TCAGCGGTGTGATCTTCAATGCC	
SMG7-qF1	GCAGAGGGGGATTCCAGGAGCA	qRT-PCR for AT5G19400 (*SMG7*) and
SMG7-qR1	TTGCAAGCTGATGATGTGGGTTTCC	*SMG7-ΔUTR* cDNA
BARENTSZ1 AT1G80000.1+2-qF1	TGGTTCTTACCAAGCAGACAAACC	qRT-PCR for AT1G80000 (*BARENTSZ1*)
BARENTSZ1 AT1G80000.1+2-qR1	TGGAACTGTTCTCTTGGCTGGAC	
PTB2-PTC-qF1	TGTCTTGCATCTGGTATTCTCAGC	qRT-PCR for AT5G53180 PTC– splice
PTB2-PTC-R1	TGCTTGGTATCCGGCTGTCTTC	variant
PTB2+PTC-qF1	TCGAAGGCGATGATGCTCGTATG	qRT-PCR for AT5G53180 PTC+ splice
PTB2+PTC-qF1	TTGCCTTGACATGGCCCAGATG	variant
AT4G36960-PTC-qF1	AGAGATTTCAAAAGGAGGAAGAGG	qRT-PCR for AT4G36960 PTC– splice
AT4G36960-PTC-qR1	GAAACCCTAACACACTCAAAAAG	variant (Drechsel et al., 2013)
AT4G36960+PTC-qF1	GAAAGAGATGTGCTTGTGGTTTG	qRT-PCR for AT4G36960 PTC+ splice
AT4G36960+PTC-qR1	GAAACCCTAACACACTCAAAAAG	variant (Drechsel et al., 2013)
FRK1-qF1	ATCTTCGCTTGGAGCTTCTC	qRT-PCR for *FRK1*
FRK1-qR1	TGCAGCGCAAGGACTAGAG	
WRKY29-qF1	ATCCAACGGATCAAGAGCTG	qRT-PCR for *WRKY29* (Denoux et al.,
WRKY29-qR1	GCGTCCGACAACAGATTCTC	2008)

Extended Experimental Procedures

Plant material

The *eds1-2* (Bartsch et al., 2006), *pad4-1* (Jirage et al., 1999), *sgt1b (eta3)* (Gray et al., 2003), *rar1-21* (Tornero et al., 2002), *sid2-1* (Nawrath and Métraux, 1999), *fls2* (SALK_093905) (Heese et al., 2007), and *smg7-1* mutant lines (Riehs et al., 2008), which all were in Col background, were published previously. *Gcn2-2* seeds were a gift from Jean-Marc Deragon, *sid2-1* seeds were a gift from Paul Schulze-Lefert, and Genetrap line GT8359 (L*er* background) was obtained from Cold Spring Harbor Laboratory. Stable transgenic *SMG7-ΔUTR* cDNA transformants and *RPS6*^{Ler} transformants were generated by cloning of the corresponding cDNA or genomic region (including 1.5 kb of upstream promoter region) into the binary vectors pCBM10 (encoding for actin promoter and nopaline synthase terminator) or pCBK5 (Riha et al., 2002), respectively, followed by *Agrobacterium*-mediated transformation using the floral-dip method. Plants used for *REX*-mapping were generated by standard genetic crosses of Col-*smg7* to L*er* and subsequent backcrosses to L*er*. Genetic markers used for mapping are listed in Table S4.

Measurement of ROS generation

Reactive oxygen species (ROS) detection was monitored by a luminol-based assay on leaf disc samples (Keppler et al., 1989). Leaf discs (diameter = 4 mm) were cut with a cork borer from 5-week-old short day (8 hours photoperiod, 21°C) grown plants and incubated in 150 µL of sterile water in 96-well plates (Thermo Fisher) over night. The water was then replaced by a solution containing 17 mg/mL of the luminol derivate L-012 (Wako Chemicals), 10 mg/mL horseradish peroxidase (Sigma) and 100 nM flg22. Luminescence, expressed as relative light units (RLU) was than recorded over 40 min using a Synergy 4 multimode plate reader (Biotek).

Salicylic acid quantification

Free and total levels of salicylic acid were measured by high-performance anion-exchange chromatography as previously described (Rozhon et al., 2005).

Chlorsulfuron treatment

Seedlings were germinated on 0.5x Murashige and Skoog (MS) agar (supplemented with Gamborg vitamins) and were grown for 12 days with 16/8h photoperiod. Twenty-four hours before treatment, seedlings were carefully transferred into 6-well plates supplemented with 4 mL liquid 0.5 x MS medium. On the next day, seedlings were treated with 0.6 µM chlorsulfuron (Sigma) for 7 hours to induce amino acid starvation (Lageix et al., 2008). The seedlings were then harvested and flash frozen in liquid nitrogen for subsequent RNA and protein analysis.

Protein analysis

For total protein extraction, approximately 0.1 g seedlings were ground in liquid nitrogen. An equal volume of ice-cold Lacus buffer (25mM Tris pH 7.8, 75 mM NaCl, 10 mM MgCl2, 15 mM EGTA, 1 mM dithiothreitol, 1 mM NaF, 0.5 mM NaVO$_3$, 15 mM beta-glycerophosphate, 15 mM p-nitrophenylphosphate, 0.1% Tween-20, 0.5 mM phenylmethylsulfonyl fluoride, 5 µg/mL leupeptin, and 5µg/mL aprotinin), supplemented with protease inhibitor cocktail (complete Mini, Roche) and phosphatase inhibitor (phosSTOP, Roche) was added, followed by brief extraction on a vortex mixer. The sample debris was then removed by two centrifugation steps (30 min at 12000 rpm, 10 min at 12000 rpm, 4°C). The remaining supernatant was mixed with 5xLaemmli buffer and was separated on a 12% SDS-PAGE gel. Phosphorylation of eIF2α was detected using a monoclonal phospho-specific primary antibody (clone ab23157, Abcam) at 1:500 dilution. The secondary antibody (mouse anti-rabbit HRP conjugate, Pierce #31460) was used at 1:20000. Signals were detected using a chemiluminescent substrate (ECL, Pierce) and were recorded on the Gel Doc XR System (Bio-Rad).

RNA-seq analysis

For whole transcriptome profiling of *pad4* and *smg7 pad4* mutants, three single-end (SE) second-strand specific libraries per genotype generated using the Scriptseq Complete Plant kit (Epicentre) were sequenced on the Illumina HiSeq2000 platform. Similarly, one library of *smg7* lines in L*er* background (L*er-smg7 REX*$^{Ler/Ler}$) and *SMG7* wild-type L*er* (L*er-SMG7 REX*$^{Ler/Ler}$) plants, each pooled from leaf material of three plants was prepared and sequenced as described above. For *smg7 pad4* and *pad4* RNA-seq the number of RNA-seq reads generated ranged from 52 to 67 million reads. Reads were mapped to the *Arabidopsis thaliana* reference genome TAIR10 (*http://www.arabidopsis.org*) using *Tophat v2.0.8b* (Trapnell et al., 2009) by allowing a maximum of three mismatches. In order to filter genes that are not expressed, reads per kilobase of transcript per million reads mapped (RPKM) values per gene per library were computed by using gene length from the representative gene model. Genes with RPKM≥1 in at least three out of six libraries were alone considered expressed and retained for differential gene expression analysis. Counts per gene from the retained genes were then provided to the R/bioconductor package DESeq v1.10.1 (Anders and Huber, 2010) to detect differentially expressed genes between *pad4 and smg7 pad4*. Cutoffs of *q≤0.05* were taken as the criterion for significant differential gene expression. GO term analysis was carried out using the GO annotation search tool on TAIR. For RNA-seq analysis of L*er-smg7 REX*$^{Ler/Ler}$ and L*er-SMG7 REX*$^{Ler/Ler}$ reads were mapped to the L*er* genome scaffold (Schneeberger et al., 2011) and were quantified using CLC Genomics Workbench 5.5.1 and custom-made Perl scripts. Read densities were visualized using Integrated Genome Browser (Nicol et al., 2009). Illumina RNA-seq data sets (Table S1) were deposited at GEO (GSE55884).

Supplemental References

Anders, S., and Huber, W. (2010). Differential expression analysis for sequence count data. Genome Biol. *11*, R106.

Denoux, C., Galletti, R., Mammarella, N., Gopalan, S., Werck, D., De Lorenzo, G., Ferrari, S., Ausubel, F.M., and Dewdney, J. (2008). Activation of defense response pathways by OGs and Flg22 elicitors in Arabidopsis seedlings. Mol Plant *1*, 423–445.

Gray, W.M., Muskett, P.R., Chuang, H.-W., and Parker, J.E. (2003). Arabidopsis SGT1b is required for SCF(TIR1)-mediated auxin response. Plant Cell *15*, 1310–1319.

Heese, A., Hann, D.R., Gimenez-Ibanez, S., Jones, A.M.E., He, K., Li, J., Schroeder, J.I., Peck, S.C., and Rathjen, J.P. (2007). The receptor-like kinase SERK3/BAK1 is a central regulator of innate immunity in plants. Proc. Natl. Acad. Sci. U.S.a. *104*, 12217–12222.

Jirage, D., Tootle, T.L., Reuber, T.L., Frost, L.N., Feys, B.J., Parker, J.E., Ausubel, F.M., and Glazebrook, J. (1999). Arabidopsis thaliana PAD4 encodes a lipase-like gene that is important for salicylic acid signaling. Proc. Natl. Acad. Sci. U.S.a. *96*, 13583–13588.

Keppler, L.D., Baker, C.J., and Atkinson, M.M. (1989). Active oxygen production during a bacteria-induced hypersensitive reaction in tobacco suspension cells. Phytopathology.

Lageix, S., Lanet, E., Pouch-Pélissier, M.-N., Espagnol, M.-C., Robaglia, C., Deragon, J.-M., and Pélissier, T. (2008). Arabidopsis eIF2alpha kinase GCN2 is essential for growth in stress conditions and is activated by wounding. BMC Plant Biol. *8*, 134.

Nawrath, C., and Métraux, J.P. (1999). Salicylic acid induction-deficient mutants of Arabidopsis express PR-2 and PR-5 and accumulate high levels of camalexin after pathogen inoculation. Plant Cell *11*, 1393–1404.

Nicol, J.W., Helt, G.A., Blanchard, S.G., Raja, A., and Loraine, A.E. (2009). The Integrated Genome Browser: free software for distribution and exploration of genome-scale datasets. Bioinformatics *25*, 2730–2731.

Riha, K., Watson, J.M., Parkey, J., and Shippen, D.E. (2002). Telomere length deregulation and enhanced sensitivity to genotoxic stress in Arabidopsis mutants deficient in Ku70. Embo J. *21*, 2819–2826.

Rozhon, W., Petutschnig, E., Wrzaczek, M., and Jonak, C. (2005). Quantification of free and total salicylic acid in plants by solid-phase extraction and isocratic high-performance anion-exchange chromatography. Anal Bioanal Chem *382*, 1620–1627.

Schneeberger, K., Ossowski, S., Ott, F., Klein, J.D., Wang, X., Lanz, C., Smith, L.M., Cao, J., Fitz, J., Warthmann, N., et al. (2011). Reference-guided assembly of four diverse Arabidopsis thaliana genomes. Proc. Natl. Acad. Sci. U.S.a. 108, 10249–10254.

Staiger, D., and Brown, J.W.S. (2013). Alternative splicing at the intersection of biological timing, development, and stress responses. Plant Cell *25*, 3640–3656.

Tornero, P., Merritt, P., Sadanandom, A., Shirasu, K., Innes, R.W., and Dangl, J.L. (2002). RAR1 and NDR1 contribute quantitatively to disease resistance in Arabidopsis, and their relative contributions are dependent on the R gene assayed. Plant Cell *14*, 1005–1015.

Trapnell, C., Pachter, L., and Salzberg, S.L. (2009). TopHat: discovering splice junctions with RNA-Seq. Bioinformatics *25*, 1105–1111.